Light scattering by optically anisotropic scatterers: *T*-matrix theory for radial and uniform anisotropies

A. D. Kiselev,[1,*] V. Yu. Reshetnyak,[2,†] and T. J. Sluckin[3,‡]
[1]*Chernigov State Technological University, Shevchenko Street 95, 14027 Chernigov, Ukraine*
[2]*Kiev University, Prospect Glushkova 6, 03680 Kiev, Ukraine*
[3]*Faculty of Mathematical Studies, University of Southampton, Southampton SO17 1BJ, United Kingdom*
(Received 12 September 2001; revised manuscript received 21 December 2001; published 3 May 2002)

We extend the *T*-matrix approach to light scattering by spherical particles to some simple cases in which the scatterers are optically anisotropic. Specifically, we consider cases in which the spherical particles include radially and uniformly anisotropic layers. We find that in both cases the *T*-matrix theory can be formulated using a modified *T*-matrix ansatz with suitably defined modes. In a uniformly anisotropic medium we derive these modes by relating the wave packet representation and expansions of electromagnetic field over spherical harmonics. The resulting wave functions are deformed spherical harmonics that represent solutions of the Maxwell equations. We present preliminary results of numerical calculations of the scattering by spherical droplets. We concentrate on cases in which the scattering is due only to the local optical anisotropy within the scatterer. For radial anisotropy we find that nonmonotonic dependence of the scattering cross section on the degree of anisotropy can occur in a regime to which both the Rayleigh and semiclassical theories are inapplicable. For uniform anisotropy the cross section is strongly dependent on the angle between the incident light and the optical axis, and for larger droplets this dependence is nonmonotonic.

DOI: 10.1103/PhysRevE.65.056609 PACS number(s): 42.25.Fx, 77.84.Nh

I. INTRODUCTION

The problem of light scattering by particles of one medium embedded in another has a long history, dating back almost a century to the classical exact solution by Mie [1]. The Mie solution applies to scattering by uniform spherical particles with isotropic dielectric properties. More recently, this strategy has been successfully applied to ellipsoidal particles and some circumstances in which the dielectric tensor is anisotropic [2–8].

There are a large number of physical contexts in which it is useful to understand light scattering by impurities [9]. A particular example of recent interest concerns liquid crystal devices. There are now a number of systems in which liquid crystal droplets are suspended in a polymer matrix—the so-called polymer dispersed liquid crytal (PDLC) systems—or the inverse system, involving colloids now with a nematic liquid crystal solvent. These inverse systems are commonly known as filled nematics [10,11].

In such systems one needs to calculate light scattering by composite anisotropic particles embedded in an isotropic or an anisotropic matrix. The model scatterer usually consists of a small central isotropic particle (''the core''), coated by a much larger region in which the optical tensor is anisotropic. This is equivalent to examining light scattering by a composite particle consisting of the central core plus a surrounding liquid crystalline layer.

A number of approaches are available to study light scattering by complex objects. A brief summary is as follows. The scattering amplitudes can be described using Green's function techniques [12], but these involve solving complex integral equations over infinite domains. Under some circumstances one can approximate the kernels of these equations either as the incident wave or as a semiclassical perturbed wave, leading to the well-known Rayleigh-Gans (RG) and anomalous diffraction approximations (ADA). These have been used by Žumer and co-workers to examine the problems we consider in this paper [13,14]. However, the approximations are only valid over certain wavelength and optical contrast regimes. The century-old Mie strategy and its modern *T*-matrix extensions yield exact solutions, but unfortunately this approach does not work in every case. Finally, one can of course use real space finite element approaches. However, in order to be efficient and accurate, these have to be very computationally intensive. In particular, without significant increase in computational power, this type of approach will probably not be adequate to discuss scattering in complex many-particle systems. For a more comprehensive review we refer the reader to Chap. 2 in Ref. [15] and references therein.

The analysis of a Mie-type theory uses a systematic expansion of the electromagnetic field over vector spherical harmonics. The specific form of the expansions is known as the *T*-matrix ansatz [16]. The *T*-matrix theory is known to be a computationally efficient approach to study light scattering by nonspherical optically isotropic particles [15]. One may thus expect that a *T*-matrix approach to geometrically spherical but optically nonspherical scatterers can at the very least enable scattering properties to be evaluated when the approximate methods cannot be applied. In addition, whereas the region of validity of the approximate methods such as RG and ADA in the case of isotropic scatterers is reasonably well understood, in the case of anisotropic scatterers this problem has not been studied in any detail.

*Email address: kisel@elit.chernigov.ua
†Email address: reshet@iop.kiev.ua
‡Email address: t.j.sluckin@maths.soton.ac.uk

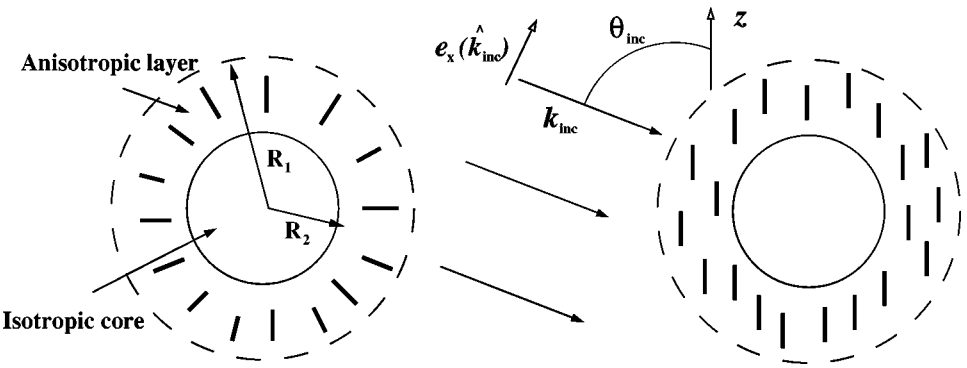

FIG. 1. Distributions of optical axis in the anisotropic layer around a spherical particle for radial and uniform structures. The angle of incidence θ_{inc} is the angle between the direction of incidence $\hat{\mathbf{k}}$ and the direction of the uniform anisotropy. The polarization vector $\mathbf{e}_y(\hat{\mathbf{k}}_{inc})$ is normal to the plane of the picture, $\mathbf{e}_y(\hat{\mathbf{k}}_{inc}) \propto \hat{\mathbf{k}}_{inc} \times \hat{\mathbf{z}}$. Inside the uniformly anisotropic layer plane waves linearly polarized along $\mathbf{e}_y(\hat{\mathbf{k}}_{inc})$ represent ordinary waves.

Recently, in Refs. [7,8] we have studied the scattering problem for the optical axis distributions of the form: $n_r\hat{\mathbf{r}} + n_\vartheta\hat{\boldsymbol{\vartheta}} + n_\varphi\hat{\boldsymbol{\varphi}}$. By using separation of variables and expansions over vector spherical harmonics, we have developed the generalized Mie theory as an extension of the *T*-matrix ansatz [16]. This theory combines computational efficiency of the *T*-matrix approach and well defined transformation properties of the spherical harmonics under rotations. In this paper we discuss this theory in more detail and explain how this approach can be extended to the case of uniformly anisotropic spherical particles.

The layout of the paper is as follows. General discussion of the model is given in Sec. II. Then in Sec. III we outline the *T*-matrix formalism for the isotropic medium in the form suitable for subsequent generalization. In Sec. IV, as the simplest case to start from, we consider how the *T*-matrix ansatz applies for the radially anisotropic layer. We find that the structure of electromagnetic modes in the layer requires modification of the standard *T*-matrix ansatz. In Sec. V we describe the method to put the scattering problem into the language of *T*-matrix by linking the representations of plane wave packets and of spherical harmonics. For uniformly anisotropic scatterer we define generalized spherical harmonics and show that the effect of angular momentum mixing can be treated efficiently. In Sec. VI we make brief comments on the numerical strategy and present some numerical results for the total scattering cross section in the limiting case of a droplet, i.e., when the radius of the isotropic core of the scatterer is negligible. Anisotropy effects are our primary concern and for this reason we pay special attention to the special case for which the ordinary wave refractive index and the refractive index of the material are matched. In addition, we emphasize the importance of anisotropy effects by making comparison between angular distributions of scattered wave intensities for radially anisotropic layers and effective isotropic layers of the same scattering efficiency. Finally, in Sec. VII we present our results and make some concluding remarks. Details on some technical results are relegated to Appendixes A–C.

II. MODEL

We consider scattering by a spherical particle of radius R_1 embedded in a uniform isotropic dielectric medium with dielectric constant $\epsilon_{ij} = \epsilon\delta_{ij}$ and magnetic permeability $\mu_{ij} = \mu\delta_{ij}$. The scattering particle consists of an inner isotropic core of radius R_2, surrounded by an anisotropic annular layer of thickness $d = R_1 - R_2$.

Within the inner core of the scatterer the dielectric tensor $\boldsymbol{\epsilon}$, and the magnetic permittivity μ take the values $\boldsymbol{\epsilon}_{ij} = \epsilon_2\delta_{ij}$, $\boldsymbol{\mu}_{ij} = \mu_2\delta_{ij}$. The dielectric tensor within the annular layer is locally uniaxial. The optical axis distribution is defined by the vector field $\hat{\mathbf{n}}$. (Carets will denote unit vectors.) Then within the annular layer $\boldsymbol{\epsilon}_{ij}(\mathbf{r}) = \epsilon_1\delta_{ij} + \Delta\epsilon_1(\hat{\mathbf{n}}(\mathbf{r}) \otimes \hat{\mathbf{n}}(\mathbf{r}))_{ij}$ and $\boldsymbol{\mu}_{ij} = \mu_1\delta_{ij}$. The unit vector $\hat{\mathbf{n}}$ corresponds to a liquid crystal director for material within the annular region with $\epsilon_1 = \epsilon_\perp$ and $\Delta\epsilon_1 = \epsilon_\parallel - \epsilon_\perp$.

We shall suppose that the director field can be written in one of the following forms: $\hat{\mathbf{n}} = \hat{\mathbf{z}}$ or $\hat{\mathbf{n}} = \hat{\mathbf{r}}$, where $\hat{\mathbf{r}} = (\sin\theta\cos\phi, \sin\theta\sin\phi, \cos\theta)$ is the unit radial vector; ϕ and θ are Euler angles of the unit vector $\hat{\mathbf{r}}$; $\hat{\mathbf{x}}$, $\hat{\mathbf{y}}$, and $\hat{\mathbf{z}}$ are the unit vectors directed along the corresponding coordinate axes.

In Fig. 1 we have shown these director distributions. Figure 1(a) shows the radial (and spherically symmetric) director distribution. Light scattering from the radially anisotropic annular layer was first studied long ago by Roth and Digman [3] using the technique normally known as Debye potentials. In this case the spherical symmetry of the problem plays an important role in rendering the Maxwell equations soluble. In an earlier paper [8] we have recovered this solution as a special case of a more general set of anisotropies. A crucial step in the derivation of this result involves writing the so-called modified *T*-matrix ansatz.

We show in Fig. 1(b) the case in which the optical axis is directed along the *z* axis and is uniformly distributed within the annular layer. The case where the scatterer is a long cylinder parallel to $\hat{\mathbf{n}}$ presents no difficulties and can be treated in cylindrical coordinate system [17]. Scattering from spherical uniformly anisotropic particles is not exactly soluble [17] and has been studied by using the Rayleigh-Gans method and the anomalous diffraction approximation in Refs. [13,14].

A simple limit of the physical situations we consider puts

$\epsilon=\epsilon_1=\epsilon_2$, with $\mu=\mu_1=\mu_2$. The first condition allows us to concentrate on situations in which the scattering is governed by the anisotropic part of the dielectric properties. This distinguishes our case from other studies of scattering by spheres, in which the isotropic optical contrast dominates. However, there is also a motivation for this hypothesis in terms of liquid crystal device physics, and we shall discuss this at greater length in a subsequent paper. However, the result of the hypothesis is that the scattering by our model spheres disappears in the limit of zero anisotropy. In addition, for a uniformly anisotropic layer we shall show explicitly that the scattering process does not involve the y component of the incoming plane wave provided the refractive indices n and n_1 are matched.

III. *T*-MATRIX APPROACH IN ISOTROPIC MEDIUM

A. *T*-matrix ansatz

In this subsection we remind the reader about the relationship between Maxwell's equations in the region of a scatterer and the formulation of scattering properties in terms of the T matrix [9,12]. Our formulation is slightly nonstandard. Some technical details, which can be omitted at first reading, have been relegated to the appendixes (more details can be found in Refs. [18,19]).

We shall need to write the Maxwell equations for a harmonic electromagnetic wave (time-dependent factor is $\exp\{-i\omega t\}$) in the form:

$$-in_i[\mu_i k_i]^{-1}\nabla\times\mathbf{E}=\mathbf{H}, \tag{1a}$$

$$i\mu_i[n_i k_i]^{-1}\nabla\times\mathbf{H}=\mathbf{E}+u_i(\hat{\mathbf{n}}\cdot\mathbf{E})\hat{\mathbf{n}}, \tag{1b}$$

where $n_i=\sqrt{\epsilon_i\mu_i}$ are refractive indexes for the regions, where $R_2<r<R_1$ $(i=1)$ and $r<R_2$ $(i=2)$; $k_i=n_i k_{vac}$ ($k_{vac}=\omega/c=2\pi/\lambda$ is the free-space wave number). We define the *anisotropy parameter* as $u_1=\Delta\epsilon_1/\epsilon_1$ (in the annular layer). Then inside the isotropic core $u_2=0$. Finally, for brevity, in the region outside the scatterer $r>R_1$, the index will be suppressed, giving $k\equiv nk_{vac}$ and $u=0$.

The electromagnetic field can always be expanded using the vector spherical harmonic basis, $\mathbf{Y}_{j+\delta\,j\,m}(\phi,\theta)\equiv\mathbf{Y}_{j+\delta\,j\,m}(\hat{\mathbf{r}})$ $(\delta=0,\pm1)$ [20], as follows:

$$\mathbf{E}=\sum_{jm}\mathbf{E}_{jm}=\sum_{\substack{jm\\ \alpha=o,e,m}}p_{jm}^{(\alpha)}(r)\mathbf{Y}_{jm}^{(\alpha)}(\hat{\mathbf{r}}), \tag{2a}$$

$$\mathbf{H}=\sum_{jm}\mathbf{H}_{jm}=\sum_{\substack{jm\\ \alpha=o,e,m}}q_{jm}^{(\alpha)}(r)\mathbf{Y}_{jm}^{(\alpha)}(\hat{\mathbf{r}}), \tag{2b}$$

where $\mathbf{Y}_{jm}^{(m)}$, $\mathbf{Y}_{jm}^{(e)}$, and $\mathbf{Y}_{jm}^{(o)}$ are magnetic, electric, and longitudinal harmonics, respectively, defined by Eq. (A4) (a number of relations for the vector spherical harmonics used throughout this paper are considered in Appendix A). The electric field is now completely described by the coefficients $\{p_{jm}^{(\alpha)}(r)\}$ and similarly the magnetic field is now described by $\{q_{jm}^{(\alpha)}(r)\}$ with $\alpha=\{o,e,m\}$.

In the simplest case of an isotropic medium we can use separation of variables to derive the coefficient functions that can be expressed in terms of spherical Bessel functions, $j_j(x)=[\pi/(2x)]^{1/2}J_{j+1/2}(x)$, and spherical Hankel functions [21], $h_j^{(1)}(x)=[\pi/(2x)]^{1/2}H_{j+1/2}^{(1)}(x)$, and their derivatives as follows:

$$\mathbf{E}_{jm}=\alpha_{jm}\mathbf{M}_{jm}^{(m)}(\rho,\hat{\mathbf{r}})+\beta_{jm}\tilde{\mathbf{M}}_{jm}^{(m)}(\rho,\hat{\mathbf{r}})-\frac{\mu}{n}[\tilde{\alpha}_{jm}\mathbf{M}_{jm}^{(e)}(\rho,\hat{\mathbf{r}})+\tilde{\beta}_{jm}\tilde{\mathbf{M}}_{jm}^{(e)}(\rho,\hat{\mathbf{r}})], \tag{3a}$$

$$\mathbf{H}_{jm}=\tilde{\alpha}_{jm}\mathbf{M}_{jm}^{(m)}(\rho,\hat{\mathbf{r}})+\tilde{\beta}_{jm}\tilde{\mathbf{M}}_{jm}^{(m)}(\rho,\hat{\mathbf{r}})+\frac{n}{\mu}[\alpha_{jm}\mathbf{M}_{jm}^{(e)}(\rho,\hat{\mathbf{r}})+\beta_{jm}\tilde{\mathbf{M}}_{jm}^{(e)}(\rho,\hat{\mathbf{r}})], \tag{3b}$$

where α_{jm}, $\tilde{\alpha}_{jm}$, β_{jm}, and $\tilde{\beta}_{jm}$ are integration constants; the vector functions $\mathbf{M}_{jm}^{(\alpha)}$ and $\tilde{\mathbf{M}}_{jm}^{(\alpha)}$ are given by

$$\mathbf{M}_{jm}^{(m)}(\rho,\hat{\mathbf{r}})=j_j(\rho)\mathbf{Y}_{jm}^{(m)}(\hat{\mathbf{r}}),$$

$$\mathbf{M}_{jm}^{(e)}(\rho,\hat{\mathbf{r}})=Dj_j(\rho)\mathbf{Y}_{jm}^{(e)}(\hat{\mathbf{r}})+\frac{\sqrt{j(j+1)}}{\rho}j_j(\rho)\mathbf{Y}_{jm}^{(o)}(\hat{\mathbf{r}}), \tag{4a}$$

$$\tilde{\mathbf{M}}_{jm}^{(m)}(\rho,\hat{\mathbf{r}})=h_j^{(1)}(\rho)\mathbf{Y}_{jm}^{(m)}(\hat{\mathbf{r}}),$$

$$\tilde{\mathbf{M}}_{jm}^{(e)}(\rho,\hat{\mathbf{r}})=Dh_j^{(1)}(\rho)\mathbf{Y}_{jm}^{(e)}(\hat{\mathbf{r}})+\frac{\sqrt{j(j+1)}}{\rho}h_j^{(1)}(\rho)\mathbf{Y}_{jm}^{(o)}(\hat{\mathbf{r}}), \tag{4b}$$

where $Df(x)\equiv x^{-1}(d/dx)[xf(x)]$ and $\rho\equiv kr$.

There are two cases of Eq. (3a) that are of particular interest. They correspond to the incoming incident wave $\{\mathbf{E}_{inc},\mathbf{H}_{inc}\}$ and the outgoing scattered wave $\{\mathbf{E}_{sca},\mathbf{H}_{sca}\}$:

$$\mathbf{E}_{jm}^{(inc)}=\alpha_{jm}^{(inc)}\,\mathbf{M}_{jm}^{(m)}-\frac{\mu}{n}\tilde{\alpha}_{jm}^{(inc)}\,\mathbf{M}_{jm}^{(e)},$$

$$\mathbf{H}_{jm}^{(inc)}=\tilde{\alpha}_{jm}^{(inc)}\,\mathbf{M}_{jm}^{(m)}+\frac{n}{\mu}\alpha_{jm}^{(inc)}\,\mathbf{M}_{jm}^{(e)}, \tag{5}$$

$$\mathbf{E}_{jm}^{(sca)}=\beta_{jm}^{(sca)}\,\tilde{\mathbf{M}}_{jm}^{(m)}-\frac{\mu}{n}\tilde{\beta}_{jm}^{(sca)}\,\tilde{\mathbf{M}}_{jm}^{(e)},$$

$$\mathbf{H}_{jm}^{(sca)}=\tilde{\beta}_{jm}^{(sca)}\,\tilde{\mathbf{M}}_{jm}^{(m)}+\frac{n}{\mu}\beta_{jm}^{(sca)}\,\tilde{\mathbf{M}}_{jm}^{(e)}. \tag{6}$$

Now the incoming incident wave is characterized by amplitudes $\alpha_{jm}^{(inc)}$, $\tilde{\alpha}_{jm}^{(inc)}$ and the scattered outgoing waves are similarly characterized by amplitudes $\beta_{jm}^{(sca)}$, $\tilde{\beta}_{jm}^{(sca)}$. Our task is now to relate $\{\alpha\}$ and $\{\beta\}$.

In this regime, the polarization vector of a transverse plane wave incident in the direction specified by an unit vector $\hat{\mathbf{k}}_{inc}$ is

$$\mathbf{E}^{(inc)} = \sum_{\nu=\pm 1} E_\nu^{(inc)} \mathbf{e}_\nu(\hat{\mathbf{k}}_{inc}). \tag{7}$$

We show in Eq. (A13) the coefficients $\{\alpha\}$ of the expansion (5) takes the form:

$$\alpha_{jm}^{(inc)} \equiv \sum_{\alpha=x,y} \alpha_{jm;\,\alpha}^{(inc)} E_\alpha^{(inc)} = i\,\alpha_j \sum_{\nu=\pm 1} D_{m\nu}^{j}(\hat{\mathbf{k}}_{inc})\,\nu E_\nu^{(inc)},$$

$$\tilde{\alpha}_{jm}^{(inc)} \equiv \sum_{\alpha=x,y} \tilde{\alpha}_{jm;\,\alpha}^{(inc)} E_\alpha^{(inc)} = n/\mu\,\alpha_j \sum_{\nu=\pm 1} D_{m\nu}^{j}(\hat{\mathbf{k}}_{inc}) E_\nu^{(inc)}, \tag{8}$$

where $\alpha_j = i^{j+1}[2\pi(2j+1)]^{1/2}$, $D_{mm'}^{j}$ is the Wigner D function [20,22] and the basis vectors $\mathbf{e}_{\pm 1}(\hat{\mathbf{k}}_{inc})$ are perpendicular to $\hat{\mathbf{k}}_{inc}$ and defined by Eq. (A2).

Thus outside the scatterer the electromagnetic field is a sum of the transverse plane wave incident in the direction specified by a unit vector $\hat{\mathbf{k}}_{inc}$ ($\beta_{jm}^{(inc)} = \tilde{\beta}_{jm}^{(inc)} = 0$) and the outgoing wave with $\alpha_{jm}^{(sca)} = \tilde{\alpha}_{jm}^{(sca)} = 0$ as required by the Sommerfeld radiation condition.

So long as the scattering problem is linear, the coefficients $\beta_{jm}^{(sca)}$ and $\tilde{\beta}_{jm}^{(sca)}$ can be written as linear combinations of $\alpha_{jm}^{(inc)}$ and $\tilde{\alpha}_{jm}^{(inc)}$:

$$\beta_{jm}^{(sca)} = \sum_{j',m'} \left[T_{jm,\,j'm'}^{11}\,\alpha_{j'm'}^{(inc)} + \frac{\mu}{n} T_{jm,\,j'm'}^{12}\,\tilde{\alpha}_{j'm'}^{(inc)} \right],$$

$$\tilde{\beta}_{jm}^{(sca)} = \sum_{j',m'} \left[\frac{n}{\mu} T_{jm,\,j'm'}^{21}\,\alpha_{j'm'}^{(inc)} + T_{jm,\,j'm'}^{22}\,\tilde{\alpha}_{j'm'}^{(inc)} \right]. \tag{9}$$

These formulas define the elements of the T matrix in the most general case.

In general, the outgoing wave with angular momentum index j arises from ingoing waves of all other indices j'. In such cases we say that the scattering process mixes angular momenta [16]. The light scattering from the uniformly anisotropic scatterer, depicted in Fig. 1(b), provides an example of such a scattering process. In this case the cylindrical symmetry of the optical axis distribution causes the T matrix to be diagonal over azimuthal indices m and m': $T_{jm,\,j'm'}^{nn'} = \delta_{mm'} T_{jj';\,m}^{nn'}$. Then we can conveniently rewrite the relation (9) using matrix notations:

$$\boldsymbol{\beta}_{jm}^{(sca)} = \sum_{j'} \mathbf{T}_{jj';\,m} \boldsymbol{\alpha}_{j'm}^{(inc)}, \tag{10}$$

where

$$\mathbf{T}_{jj';\,m} = \begin{pmatrix} T_{jj';\,m}^{11} & T_{jj';\,m}^{12} \\ T_{jj';\,m}^{21} & T_{jj';\,m}^{22} \end{pmatrix},$$

$$\boldsymbol{\alpha}_{jm}^{(inc)} = \begin{pmatrix} \alpha_{jm}^{(inc)} \\ \mu/n\,\tilde{\alpha}_{jm}^{(inc)} \end{pmatrix} \quad \text{and} \quad \boldsymbol{\beta}_{jm}^{(sca)} = \begin{pmatrix} \beta_{jm}^{(sca)} \\ \mu/n\,\tilde{\beta}_{jm}^{(sca)} \end{pmatrix}.$$

In simpler scattering processes, by contrast, such angular momentum mixing does not take place. Many quantum scattering processes and classical Mie scattering belong to this category. It is seen from Fig. 1(a) that radial anisotropy keeps intact spherical symmetry of the scatterer. The radially anisotropic annular layer thus exemplifies a scatterer that does not mix angular momenta. The T matrix of a spherically symmetric scatterer is diagonal over the angular momenta and the azimuthal numbers: $T_{jj',mm'}^{nn'} = \delta_{jj'}\delta_{mm'} T_j^{nn'}$.

B. Scattering amplitude matrix

We have seen that the relation between the scattered wave (6) and the incident plane wave (5) is linear. In the far field region ($\rho \gg 1$), where the asymptotic behavior of the scattered outgoing wave is given by

$$i^{j+1}\mathbf{E}_{jm}^{(sca)} \sim \frac{e^{i\rho}}{\rho} \sum_{\nu=\pm 1} \mathbf{f}_{\nu;\,jm}, \tag{11a}$$

$$i^{j+1}\mu/n\,\mathbf{H}_{jm}^{(sca)} \sim \frac{-i\,e^{i\rho}}{\rho} \sum_{\nu=\pm 1} \nu \mathbf{f}_{\nu;\,jm}, \tag{11b}$$

$$\mathbf{f}_{\nu;\,jm} \equiv N_j\,(\mathbf{e}_\nu \cdot \boldsymbol{\beta}_{jm}^{(sca)}) D_{m\,\nu}^{j\,*}(\hat{\mathbf{k}}_{sca}) \mathbf{e}_\nu(\hat{\mathbf{k}}_{sca}),$$

with $\mathbf{e}_\nu = (-\nu, -i)/\sqrt{2}$ and $N_j = \sqrt{(2j+1)/4\pi}$, the scattering amplitude matrix $\mathbf{A}(\hat{\mathbf{k}}_{sca}, \hat{\mathbf{k}}_{inc})$, which relates $\mathbf{E}_{sca}$ and the polarization vector of the incident wave $\mathbf{E}^{(inc)}$ is defined in the following way [9,12,16]:

$$E_\nu^{(sca)} \equiv (\mathbf{e}_\nu^*(\hat{\mathbf{k}}_{sca}), \mathbf{E}_{sca}) = \frac{e^{i\rho}}{\rho} \sum_{\nu'=\pm 1} \mathbf{A}_{\nu\nu'}(\hat{\mathbf{k}}_{sca}, \hat{\mathbf{k}}_{inc}) E_{\nu'}^{(inc)}, \tag{12}$$

where an asterisk indicates complex conjugation, $\hat{\mathbf{k}}_{sca} = \hat{\mathbf{r}}$ and $\hat{\mathbf{e}}_{\pm 1}(\hat{\mathbf{k}}_{sca}) = \mp(\hat{\boldsymbol{\vartheta}} \pm i\hat{\boldsymbol{\varphi}})/\sqrt{2}$.

Equations (6), (11a) and the vector spherical harmonic relations Eqs. (A8) can now be combined to yield the expression for the scattering amplitude matrix in terms of the T matrix:

$$\begin{aligned} \mathbf{A}_{\nu\nu'}(\hat{\mathbf{k}}_{sca}, \hat{\mathbf{k}}_{inc}) = -\frac{i}{2} \sum_{jm} \sum_{j'm'} & [(2j+1)(2j'+1)]^{1/2} D_{m\nu}^{j\,*}(\hat{\mathbf{k}}_{sca}) D_{m'\nu'}^{j'}(\hat{\mathbf{k}}_{inc}) \\ & \times [\nu\nu' T_{jm,\,j'm'}^{11} - i\nu T_{jm,\,j'm'}^{12} \\ & + i\nu' T_{jm,\,j'm'}^{21} + T_{jm,\,j'm'}^{22}]. \end{aligned} \tag{13}$$

All scattering properties of the system can be computed from the elements of the scattering amplitude matrix. In Eq. (13) we see that this can be defined in terms of the elements of the T matrix defined in Eq. (9). Thus computation of these matrix elements is of crucial importance.

C. Scattering efficiency

In order to find the total scattering cross section C_{sca} we need to calculate the flux of Poynting vector of the scattered wave $\mathbf{S}^{(sca)}=c/(8\pi)\mathrm{Re}(\mathbf{E}_{sca}\times\mathbf{H}^{*}_{sca})$ through a sphere of sufficiently large radius and divide the result by $|\mathbf{S}^{(inc)}|$.

Using the expressions (11) and the orthogonality relation (A9), we can deduce the result for the total scattering cross section:

$$C_{sca}=k^{-2}I_{inc}^{-1}\sum_{jm}[\boldsymbol{\beta}_{jm}^{(sca)}]^{\dagger}\boldsymbol{\beta}_{jm}^{(sca)}, \tag{14}$$

where $I_{inc}=\Sigma_{\nu=\pm1}|E_{\nu}^{(inc)}|^2$ and the superscript † indicates Hermitian conjugation. We can now relate the scattering cross section and the elements of the T matrix. More precisely, we consider the scattering efficiency Q that is the ratio of C_{sca} and area of the composite particle $S=\pi R_1^2$.

Equations (8), (10), and (14) can now be combined to yield the expression for the scattering efficiency of a uniformly anisotropic scatterer in the following form:

$$Q=I_{inc}^{-1}\sum_{\substack{\alpha=x,y,\\ \beta=x,y}}Q_{\alpha\beta}E_{\alpha}^{(inc)}E_{\beta}^{(inc)\,*}, \tag{15}$$

$$(kR_1)^2\pi\,Q_{\alpha\beta}=\sum_{jm}[\boldsymbol{\beta}_{jm;\,\beta}^{(sca)}]^{\dagger}\boldsymbol{\beta}_{jm;\,\alpha}^{(sca)}, \tag{16}$$

$$\boldsymbol{\beta}_{jm;\,\alpha}^{(sca)}=\sum_{j'}\mathbf{T}_{jj';\,m}\boldsymbol{\alpha}_{j'm;\,\alpha}^{(inc)}. \tag{17}$$

So, we have the scattering efficiency tensor $Q_{\alpha\beta}$, which is, in general, nondiagonal and depend on incident wave angles.

For a spherically symmetric scatterer this tensor is diagonal and independent of $\hat{\mathbf{k}}_{inc}$. In this case the T matrix is diagonal and from Eqs. (15)–(17) we have the known result [16]:

$$Q_{\alpha\beta}=\frac{2\,\delta_{\alpha\beta}}{k^2R_1^2}\sum_{j=1}^{\infty}\sum_{m,n=1}^{2}(2j+1)|T_j^{mn}|^2. \tag{18}$$

In order to characterize angular distribution of scattered light intensity let us suppose that the incident wave is linearly polarized and is propagating along the z axis, $\hat{\mathbf{k}}_{inc}=\hat{\mathbf{z}}$. The wave vectors $\hat{\mathbf{k}}_{inc}$ and $\hat{\mathbf{k}}_{sca}$ define the scattering plane. For diagonal T matrix Eqs. (12) and (13) give the amplitudes of the scattered wave components that are parallel ($E_x^{(sca)}$) and normal ($E_y^{(sca)}$) to the scattering plane:

$$|E_x^{(sca)}|^2(\theta_{sca})=I_{inc}i_{\parallel}(\theta_{sca})\cos^2\psi, \tag{19a}$$

$$|E_y^{(sca)}|^2(\theta_{sca})=I_{inc}i_{\perp}(\theta_{sca})\sin^2\psi, \tag{19b}$$

$$i_{\parallel,\,\perp}=|i_1\pm i_{-1}|^2, \tag{19c}$$

$$i_{\pm1}(\theta_{sca})=(kR_1)^{-1}\sum_{j}(j+1/2)d^{j}_{1,\,\pm1}(\theta_{sca})[T_j^{11}\pm T_j^{22}], \tag{19d}$$

where ψ is the angle between the polarization vector of the incident wave and the scattering plane.

In Sec. VI A we shall use the intensity $i_{sca}(\theta_{sca})$,

$$i_{sca}(\theta_{sca})=[i_{\parallel}(\theta_{sca})+i_{\perp}(\theta_{sca})]/2, \tag{20}$$

and the factor characterizing the degree of depolarization (depolarization factor) $P_{dep}(\theta_{sca})$,

$$P_{dep}(\theta_{sca})=1-\frac{|i_{\parallel}(\theta_{sca})-i_{\perp}(\theta_{sca})|}{i_{\parallel}(\theta_{sca})+i_{\perp}(\theta_{sca})} \tag{21}$$

as quantities characterizing angular distribution and polarization of the scattered wave [23]. Note that averaging $i_{sca}(\theta_{sca})$ over the scattering angle gives the scattering efficiency:

$$Q=\int_0^{\pi}i_{sca}(\theta_{sca})\sin\theta_{sca}\,d\theta_{sca}.$$

IV. SCATTERING FROM RADIALLY ANISOTROPIC LAYER

In Sec. III A we started from the general expansion for electromagnetic field over the vector spherical harmonics (2). Then the fields in isotropic medium were expressed in terms of the modes, $\mathbf{M}_{jm}^{(\alpha)}$ and $\tilde{\mathbf{M}}_{jm}^{(\alpha)}$ [see Eq. (4)]. This expression is known as the T matrix ansatz [15,16].

We shall write down the results for electromagnetic field within the radially anisotropic layer as they are given in Ref. [8]. These can be written in the form similar to the T-matrix ansatz:

$$\mathbf{E}_{jm}=\alpha_{jm}\mathbf{P}_{jm}^{(m)}+\beta_{jm}\tilde{\mathbf{P}}_{jm}^{(m)}-\frac{\mu}{n}(\tilde{\alpha}_{jm}\mathbf{P}_{jm}^{(e)}+\tilde{\beta}_{jm}\tilde{\mathbf{P}}_{jm}^{(e)}), \tag{22a}$$

$$\mathbf{H}_{jm}=\tilde{\alpha}_{jm}\mathbf{Q}_{jm}^{(m)}+\tilde{\beta}_{jm}\tilde{\mathbf{Q}}_{jm}^{(m)}+\frac{n}{\mu}(\alpha_{jm}\mathbf{Q}_{jm}^{(e)}+\beta_{jm}\tilde{\mathbf{Q}}_{jm}^{(e)}). \tag{22b}$$

For radial anisotropy the modes that enter Eqs. (22) are given by

$$\mathbf{P}_{jm}^{(m)}=\mathbf{M}_{jm}^{(m)}(\rho_1,\hat{\mathbf{r}}), \tag{23a}$$

$$\mathbf{Q}_{jm}^{(e)}=\mathbf{M}_{jm}^{(e)}(\rho_1,\hat{\mathbf{r}}), \tag{23b}$$

$$\mathbf{Q}_{jm}^{(m)}=j_{\tilde{j}}(\rho_1)\,\mathbf{Y}_{jm}^{(m)}(\hat{\mathbf{r}}), \tag{23c}$$

$$\mathbf{P}_{jm}^{(e)}=Dj_{\tilde{j}}(\rho_1)\,\mathbf{Y}_{jm}^{(e)}(\hat{\mathbf{r}})+[\tilde{j}(\tilde{j}+1)]^{1/2}\rho_1^{-1}j_{\tilde{j}}(\rho_1)\,\mathbf{Y}_{jm}^{(o)}(\hat{\mathbf{r}}), \tag{23d}$$

where $\tilde{j}(\tilde{j}+1)=j(j+1)/(1+u_1)$ and $\rho_i\equiv k_ir$.

In the following section we shall find that the fields in uniformly anisotropic medium can also be written in the form (22). However, the expressions for the normal modes in this case will differ from those of Eqs. (23). In both cases the modes represent solutions of Maxwell's equations and turn into the isotropic medium modes (4) in the limit of small anisotropy parameter, $u\to0$.

The radial anisotropy harmonics (22) do not involve angular momentum mixing and as such they only have contributions proportional to vector spherical harmonics with angular momentum numbers given j and m. The important difference between the two cases lies in the fact that for the uniformly anisotropic layer this is no longer true.

The fields inside the isotropic core of the particle similarly also involve no angular momentum mixing:

$$\mathbf{E}_{jm}^{(c)}=\alpha_{jm}^{(c)}\,\mathbf{M}_{jm}^{(m)}-\frac{\mu_2}{n_2}\tilde{\alpha}_{jm}^{(c)}\,\mathbf{M}_{jm}^{(e)}, \tag{24a}$$

$$\mathbf{H}_{jm}^{(c)}=\tilde{\alpha}_{jm}^{(c)}\,\mathbf{M}_{jm}^{(m)}+\frac{n_2}{\mu_2}\alpha_{jm}^{(c)}\,\mathbf{M}_{jm}^{(e)}, \tag{24b}$$

where $\mathbf{M}_{jm}^{(e,m)}=\mathbf{M}_{jm}^{(e,m)}(\rho_2,\hat{\mathbf{r}})$ and $\rho_2\equiv k_2 r$.

We now pass on to the calculation of the scattering cross section using the T-matrix method. The formulas presented in this subsection form a key element in the input to this calculation.

A. *T* matrix: radial anisotropy

In order to calculate the elements of T matrix, we need to use continuity of the tangential components of the electric and magnetic fields as boundary conditions at $r=R_2$ and $r=R_1$. Equivalently, the functions $p_{jm}^{(\alpha)}\equiv\langle\mathbf{Y}_{jm}^{(\alpha)*}\cdot\mathbf{E}\rangle_{\hat{\mathbf{r}}}$, and $q_{jm}^{(e)}\equiv\langle\mathbf{Y}_{jm}^{(\alpha)*}\cdot\mathbf{H}\rangle_{\hat{\mathbf{r}}}$, $\alpha=m,e$, must be continuous at each boundary:

$$p_{jm}^{(\alpha)}(R_i+0)=p_{jm}^{(\alpha)}(R_i-0),$$
$$q_{jm}^{(\alpha)}(R_i+0)=q_{jm}^{(\alpha)}(R_i-0),\qquad i=1,2. \tag{25}$$

For the radially anisotropic distribution different angular momentum are decoupled. We have shown elsewhere that the T matrix can be computed in the closed form [8], and here we shall comment on this calculation (for more details see Ref. [18]).

Expressions for $\{p_{jm}^{(\alpha)},q_{jm}^{(\alpha)}\}$ in the ambient medium have been given implicitly in Eqs. (5) and (6). Similar expressions in the annular layer have been given by Eqs. (22) and (23). Finally, the analogous expressions inside the isotropic core have been given in Eq. (24).

In order to determine the T matrix we shall insert these expressions into the boundary conditions (25). This will yield a system of eight linear algebraic equations for the ten quantities: $\alpha_{jm}^{(inc)}$, $\tilde{\alpha}_{jm}^{(inc)}$, $\beta_{jm}^{(sca)}$, $\tilde{\beta}_{jm}^{(sca)}$, α_{jm}, β_{jm}, $\tilde{\alpha}_{jm}$, $\tilde{\beta}_{jm}$, $\alpha_{jm}^{(c)}$, and $\tilde{\alpha}_{jm}^{(c)}$. After eliminating all internal variables we shall be left with two equations in the four unknowns: $\alpha_{jm}^{(inc)}$, $\tilde{\alpha}_{jm}^{(inc)}$, $\beta_{jm}^{(sca)}$, and $\tilde{\beta}_{jm}^{(sca)}$. These equations will define the T matrix.

In order to carry out this procedure efficiently we combine Eqs. (2) and (22) by using the compact matrix notation for the components inside the anisotropic layer:

$$\begin{pmatrix} p_{jm}^{(m)}(r)\\ q_{jm}^{(e)}(r)\\ q_{jm}^{(m)}(r)\\ p_{jm}^{(e)}(r)\end{pmatrix}=\mathbf{R}^j(r)\begin{pmatrix}\alpha_{jm}\\ \beta_{jm}\\ \tilde{\alpha}_{jm}\\ \tilde{\beta}_{jm}\end{pmatrix}, \tag{26}$$

where

$$\mathbf{R}^j(r)=\begin{pmatrix} j_j(\rho_1) & h_j^{(1)}(\rho_1) & 0 & 0\\ n_1\mu_1^{-1}Dj_j(\rho_1) & n_1\mu_1^{-1}Dh_j^{(1)}(\rho_1) & 0 & 0\\ 0 & 0 & j_{\tilde{j}}(\rho_1) & h_{\tilde{j}}^{(1)}(\rho_1)\\ 0 & 0 & -\mu_1 n_1^{-1}Dj_{\tilde{j}}(\rho_1) & -\mu_1 n_1^{-1}Dh_{\tilde{j}}^{(1)}(\rho_1)\end{pmatrix}. \tag{27}$$

We can now apply the boundary conditions at the dielectric discontinuities on the inside and outside of the anisotropic layer and solve the system of linear algebraic equations. This yields the standard general form for the relation between the amplitudes of the incoming and outgoing waves (9), with the following explicit expressions for the elements of the T matrix:

$$T_j^{11}=\frac{c_2[j_j(\rho)]_1-n/\mu\, c_1[j_j(\rho)]_1'}{n/\mu\, c_1[h_j^{(1)}(\rho)]_1'-c_2[h_j^{(1)}(\rho)]_1},$$

$$T_j^{22}=-\frac{\tilde{c}_2[j_j(\rho)]_1+\mu/n\,\tilde{c}_1[j_j(\rho)]_1'}{\mu/n\,\tilde{c}_1[h_j^{(1)}(\rho)]_1'+\tilde{c}_2[h_j^{(1)}(\rho)]_1}, \tag{28}$$

where $Df(x)|_{r=R_i}\equiv[f(x)]_i'$, $f(x)|_{r=R_i}\equiv[f(x)]_i$, and

$$\begin{pmatrix} c_1 & 0\\ c_2 & 0\\ 0 & \tilde{c}_1\\ 0 & \tilde{c}_2\end{pmatrix}=\mathbf{R}_1^j(\mathbf{R}_2^j)^{-1}\times\begin{pmatrix}[j_j(\rho_2)]_2 & 0\\ n_2\mu_2^{-1}[j_j(\rho_2)]_2' & 0\\ 0 & [j_j(\rho_2)]_2\\ 0 & -n_2^{-1}\mu_2[j_j(\rho_2)]_2'\end{pmatrix},$$
$$\mathbf{R}_i^j\equiv\mathbf{R}^j|_{r=R_i}. \tag{29}$$

We note that in this result the off-diagonal elements of the T matrix vanish: $T_j^{12}=T_j^{21}=0$. This result is quite general for spherically symmetric scatterers, and physically means that there is no coupling between transverse electric and transverse magnetic waves. Equivalently there is no depolarization scattering in this scatterer. Mathematically, the result follows because the matrix (27) is block diagonal.

V. SCATTERING FROM UNIFORMLY ANISOTROPIC LAYER

By contrast with the case of the radially anisotropic scatterer considered in the preceding section, the electromagnetic field inside the uniformly anisotropic annular layer can easily be described in terms of plane waves. Unfortunately this does not render the scattering problem soluble. The difficulty lies in satisfying the boundary conditions for a spherical scatterer using the plane wave solutions of the Maxwell equations.

The starting point of the T-matrix approach to this case involves finding a representation of the electromagnetic wave analogous to the generalized T-matrix ansatz (22). However, for symmetry reasons, the structure of the modes representing the fields in the uniformly anisotropic medium differs from that in the spherically symmetric isotropic (or a radially anisotropic) geometry. In particular, the lack of spherical symmetry implies that the angular momentum number j is no longer a good quantum number. However, the cylindrical symmetry still guarantees conservation of the azimuthal number m.

The procedure is as follows. In Sec. V A we provide methods of defining modes in a uniformly anisotropic material. These modes are: (a) solutions of the Maxwell's equations and (b) deformations of the isotropic spherical harmonics. The latter condition means that the isotropic modes Eqs. (4) are recovered in the weak anisotropy limit, $u\to 0$. Then in Sec. V B, we shall use these ''quasispherical'' wave functions to derive equations that enable the elements of T matrix to be computed.

A. Angular momentum representation in the anisotropic layer

We have seen above that solutions to Maxwell's equations can be written in two ways. Either they can be expressed as plane waves, or, using a separation of variables approach, they can be written as expansions over spherical harmonics. Deriving an expression for the T matrix will require us to make a connection between these two alternative expansions. In this subsection we carry out this task.

To do this we begin with an isotropic medium. In this special case both the spherical harmonics and the plane wave solutions are known. The result is a relation between the plane wave packets and the spherical harmonics. The procedure will then be generalized to cover the case of a uniformly anisotropic medium, so as to derive a set of ''quasispherical'' normal modes.

1. Spherical modes and plane waves in isotropic media

We start with the Maxwell's equations (1) for an isotropic medium. Wavelike solutions to these equations written in terms of spherical coordinate basis functions are given by Eqs. (3) and (4). An electromagnetic wave can alternatively be written as a superposition of plane waves:

$$\mathbf{E}=\langle \exp(i\rho\,\hat{\mathbf{k}}\cdot\hat{\mathbf{r}})[E_x(\hat{\mathbf{k}})\,\mathbf{e}_x(\hat{\mathbf{k}})+E_y(\hat{\mathbf{k}})\mathbf{e}_y(\hat{\mathbf{k}})]\rangle_{\hat{\mathbf{k}}}, \quad (30a)$$

$$\mathbf{H}=\frac{n}{\mu}\langle \exp(i\rho\,\hat{\mathbf{k}}\cdot\hat{\mathbf{r}})[E_x(\hat{\mathbf{k}})\mathbf{e}_y(\hat{\mathbf{k}})-E_y(\hat{\mathbf{k}})\mathbf{e}_x(\hat{\mathbf{k}})]\rangle_{\hat{\mathbf{k}}}, \quad (30b)$$

where $\langle f\rangle_{\hat{\mathbf{k}}}\equiv\int_0^{2\pi}d\phi_k\int_0^{\pi}\sin\theta_k d\theta_k f$.

In Appendix A we derive expressions connecting the isotropic spherical modes (4a) and the vector plane waves occurring in the superposition (30):

$$\mathbf{M}_{jm}^{(m)}(\rho,\hat{\mathbf{r}})=\gamma_j\langle e^{i\rho(\hat{\mathbf{k}}\cdot\hat{\mathbf{r}})}[D_{jm}^{(y)}{}^*(\hat{\mathbf{k}})\mathbf{e}_x(\hat{\mathbf{k}}) - iD_{jm}^{(x)}{}^*(\hat{\mathbf{k}})\mathbf{e}_y(\hat{\mathbf{k}})]\rangle_{\hat{\mathbf{k}}}, \quad (31a)$$

$$\mathbf{M}_{jm}^{(e)}(\rho,\hat{\mathbf{r}})=\gamma_j\langle e^{i\rho(\hat{\mathbf{k}}\cdot\hat{\mathbf{r}})}[iD_{jm}^{(x)}{}^*(\hat{\mathbf{k}})\mathbf{e}_x(\hat{\mathbf{k}}) + D_{jm}^{(y)}{}^*(\hat{\mathbf{k}})\mathbf{e}_y(\hat{\mathbf{k}})]\rangle_{\hat{\mathbf{k}}}, \quad (31b)$$

where $\gamma_j\equiv i^{-j}(4\pi)^{-2}\sqrt{\pi(2j+1)}$ and

$$D_{jm}^{(x,y)}(\hat{\mathbf{k}})\equiv e^{-im\,\phi_k}d_{jm}^{(x,y)}(\theta_k)=D^j_{m,-1}(\hat{\mathbf{k}}) \mp D^j_{m,1}(\hat{\mathbf{k}}), \qquad D_{jm}^{(z)}(\hat{\mathbf{k}})\equiv D^j_{m,0}(\hat{\mathbf{k}}). \quad (32)$$

These relations can be explicitly verified by substituting the expansions (A13) into the right-hand sides of Eqs. (31). The linear combinations of the modes $\mathbf{M}_{jm}^{(m)}(\rho,\hat{\mathbf{r}})$ and $\mathbf{M}_{jm}^{(e)}(\rho,\hat{\mathbf{r}})$ which enter the electromagnetic field harmonics (3) can now be expressed as a superposition of plane waves:

$$\alpha_{jm}\mathbf{M}_{jm}^{(m)}-\frac{\mu}{n}\tilde{\alpha}_{jm}\mathbf{M}_{jm}^{(e)}=\langle e^{i\rho(\hat{\mathbf{k}}\cdot\hat{\mathbf{r}})}[E_{jm}^{(x)}(\hat{\mathbf{k}})\mathbf{e}_x(\hat{\mathbf{k}}) + E_{jm}^{(y)}(\hat{\mathbf{k}})\mathbf{e}_y(\hat{\mathbf{k}})]\rangle_{\hat{\mathbf{k}}}, \quad (33a)$$

$$\tilde{\alpha}_{jm}\mathbf{M}_{jm}^{(m)}+\frac{n}{\mu}\alpha_{jm}\mathbf{M}_{jm}^{(e)}=\frac{n}{\mu}\langle e^{i\rho(\hat{\mathbf{k}}\cdot\hat{\mathbf{r}})}[E_{jm}^{(x)}(\hat{\mathbf{k}})\mathbf{e}_y(\hat{\mathbf{k}}) - E_{jm}^{(y)}(\hat{\mathbf{k}})\mathbf{e}_x(\hat{\mathbf{k}})]\rangle_{\hat{\mathbf{k}}}, \quad (33b)$$

where

$$E_{jm}^{(x)}(\hat{\mathbf{k}})=\gamma_j\left\{\alpha_{jm}\,D_{jm}^{(y)}{}^*(\hat{\mathbf{k}})-i\frac{\mu}{n}\tilde{\alpha}_{jm}\,D_{jm}^{(x)}{}^*(\hat{\mathbf{k}})\right\}, \quad (34a)$$

$$E_{jm}^{(y)}(\hat{\mathbf{k}})=-\gamma_j\left\{i\,\alpha_{jm}D_{jm}^{(x)}{}^*(\hat{\mathbf{k}})+\frac{\mu}{n}\tilde{\alpha}_{jm}D_{jm}^{(y)}{}^*(\hat{\mathbf{k}})\right\}. \quad (34b)$$

We now sum Eqs. (33) over j and m. This enables the amplitudes $E_x(\hat{\mathbf{k}})$ and $E_y(\hat{\mathbf{k}})$ in Eqs. (30) to be expressed in terms of Wigner D functions:

$$E_{x,y}(\hat{\mathbf{k}}) = \sum_{jm} E_{jm}^{(x,y)}(\hat{\mathbf{k}}). \tag{35}$$

This procedure has started from plane waves (30) and spherical harmonics (3), and finished with Eqs. (34), (35). This equation defines a basis set in the space of the angular dependent amplitudes.

In fact, we shall need to carry out the inverse process. The inverse process uses the expansions (35) to derive the expressions for the spherical modes $\mathbf{M}_{jm}^{(\alpha)}$ and $\tilde{\mathbf{M}}_{jm}^{(\alpha)}$ from superpositions of plane waves (30). The procedure works as follows.

(a) We substitute the expansions of the amplitudes $E_x(\hat{\mathbf{k}})$ and $E_y(\hat{\mathbf{k}})$ from Eqs. (35) into the superpositions (30).

(b) From the expressions for the electric (magnetic) fields we obtain the spherical modes as coefficient functions proportional to α_{jm} and $-\mu/n\tilde{\alpha}_{jm}$ ($\tilde{\alpha}_{jm}$ and $n/\mu\alpha_{jm}$).

(c) In order to deduce explicit analytical expressions for the modes, we expand the plane waves over vector spherical functions by using Eqs. (A13). We then integrate the products of Wigner D functions over the angles ϕ_k and θ_k by using the orthogonality condition (A9).

(d) Finally, the modes $\tilde{\mathbf{M}}_{jm}^{(\alpha)}$ are derived from the expressions for $\mathbf{M}_{jm}^{(\alpha)}$ by changing the Bessel functions $j_j(\rho)$ to the Hankel functions $h_j^{(1)}(\rho)$.

Note that, if a linear combination of Bessel functions $j_j(\rho)$ represents a solution of linear homogeneous differential equations (Maxwell's equations in our case), then the corresponding linear combination of Hankel functions generates another solution. This remark justifies the last step in the procedure described above.

The crucial point is that this inverse procedure can be generalized to a uniformly anisotropic medium. Thus it can be applied to superpositions of plane waves representing solutions of the Maxwell's equations in the uniformly anisotropic layer, yielding expressions for the modes used in the generalized T-matrix ansatz (22). In the following subsection we perform this generalization.

2. Wave functions in an anisotropic medium

We start with the expansion (35), and use it to derive formulas for generalized spherical harmonics in the anisotropic medium. The starting point is the well known result for plane waves [23–26]:

$$\mathbf{E} = \left\langle e^{i\rho_e(\hat{\mathbf{k}}\cdot\hat{\mathbf{r}})} E_x(\hat{\mathbf{k}}) \left[\mathbf{e}_x(\hat{\mathbf{k}}) + \frac{u\sin\theta_k}{1+u}\hat{\mathbf{z}} \right] + e^{i\rho\,(\hat{\mathbf{k}}\cdot\hat{\mathbf{r}})} E_y(\hat{\mathbf{k}})\, \mathbf{e}_y(\hat{\mathbf{k}}) \right\rangle_{\hat{\mathbf{k}}}, \tag{36a}$$

$$\mathbf{H} = \frac{n}{\mu}\left\langle e^{i\rho_e(\hat{\mathbf{k}}\cdot\hat{\mathbf{r}})} n_e^{-1} E_x(\hat{\mathbf{k}})\mathbf{e}_y(\hat{\mathbf{k}}) - e^{i\rho(\hat{\mathbf{k}}\cdot\hat{\mathbf{r}})} E_y(\hat{\mathbf{k}})\mathbf{e}_x(\hat{\mathbf{k}}) \right\rangle_{\hat{\mathbf{k}}}, \tag{36b}$$

where $n_e^2 \equiv n_e^2(\theta_k) = (1+u)/(1+u\cos^2\theta_k)$ and $\rho_e \equiv n_e(\theta_k)\rho$.

We now apply the procedure described at the end of the preceding section to the plane wave packets (36). This gives a representation of the electromagnetic field in the form of the generalized T-matrix ansatz (22). Now, however, the modes no longer take the form (23), but rather the modified form:

$$\mathbf{P}_{jm}^{(m)}(\rho,\hat{\mathbf{r}}) = \gamma_j \left\langle D_{jm}^{(y)*} e^{i\rho_e(\hat{\mathbf{k}}\cdot\hat{\mathbf{r}})} \left[\mathbf{e}_x(\hat{\mathbf{k}}) + \frac{u\sin\theta_k}{1+u}\hat{\mathbf{z}} \right] - iD_{jm}^{(x)*} e^{i\rho(\hat{\mathbf{k}}\cdot\hat{\mathbf{r}})} \mathbf{e}_y(\hat{\mathbf{k}}) \right\rangle_{\hat{\mathbf{k}}}, \tag{37a}$$

$$\mathbf{P}_{jm}^{(e)}(\rho,\hat{\mathbf{r}}) = \gamma_j \left\langle iD_{jm}^{(x)*} e^{i\rho_e(\hat{\mathbf{k}}\cdot\hat{\mathbf{r}})} \left[\mathbf{e}_x(\hat{\mathbf{k}}) + \frac{u\sin\theta_k}{1+u}\hat{\mathbf{z}} \right] + D_{jm}^{(y)*} e^{i\rho(\hat{\mathbf{k}}\cdot\hat{\mathbf{r}})}\, \mathbf{e}_y(\hat{\mathbf{k}}) \right\rangle_{\hat{\mathbf{k}}}, \tag{37b}$$

$$\mathbf{Q}_{jm}^{(m)}(\rho,\hat{\mathbf{r}}) = \gamma_j \langle -iD_{jm}^{(x)*} e^{i\rho_e(\hat{\mathbf{k}}\cdot\hat{\mathbf{r}})} n_e^{-1} \mathbf{e}_y(\hat{\mathbf{k}}) + D_{jm}^{(y)*} e^{i\rho\,(\hat{\mathbf{k}}\cdot\hat{\mathbf{r}})}\, \mathbf{e}_x(\hat{\mathbf{k}}) \rangle_{\hat{\mathbf{k}}}, \tag{37c}$$

$$\mathbf{Q}_{jm}^{(e)}(\rho,\hat{\mathbf{r}}) = \gamma_j \langle D_{jm}^{(y)*} e^{i\rho_e(\hat{\mathbf{k}}\cdot\hat{\mathbf{r}})} n_e^{-1} \mathbf{e}_y(\hat{\mathbf{k}}) + iD_{jm}^{(y)*} e^{i\rho\,(\hat{\mathbf{k}}\cdot\hat{\mathbf{r}})} \mathbf{e}_x(\hat{\mathbf{k}}) \rangle_{\hat{\mathbf{k}}}, \tag{37d}$$

where $D_{jm}^{(x,y)*} \equiv D_{jm}^{(x,y)*}(\hat{\mathbf{k}})$.

Typically, solving a scattering problem for a spherical particle requires modes to be expressed in terms of vector spherical harmonics. It thus turns out to be useful to write the wave functions (37) as expansions over vector spherical harmonics:

$$\mathbf{P}_{jm}^{(\alpha)} = \sum_{\beta} \sum_{j' \geq |m|} p_{j'j;\,m}^{(\beta,\,\alpha)}(\rho)\, \mathbf{Y}_{j'm}^{(\beta)}(\hat{\mathbf{r}}), \tag{38a}$$

$$\mathbf{Q}_{jm}^{(\alpha)} = \sum_{\beta} \sum_{j' \geq |m|} q_{j'j;\,m}^{(\beta,\,\alpha)}(\rho)\, \mathbf{Y}_{j'm}^{(\beta)}(\hat{\mathbf{r}}), \tag{38b}$$

where $\alpha \in \{m,e\}$, $\beta \in \{m,e,o\}$, and

$$p_{j'j;\,m}^{(\beta,\,\alpha)}(\rho) = \langle \mathbf{Y}_{j'm}^{(\beta)*}(\hat{\mathbf{r}}) \cdot \mathbf{P}_{jm}^{(\alpha)}(\rho,\hat{\mathbf{r}}) \rangle_{\hat{\mathbf{r}}},$$

$$q_{j'j;\,m}^{(\beta,\,\alpha)}(\rho) = \langle \mathbf{Y}_{j'm}^{(\beta)*}(\hat{\mathbf{r}}) \cdot \mathbf{Q}_{jm}^{(\alpha)}(\rho,\hat{\mathbf{r}}) \rangle_{\hat{\mathbf{r}}}. \tag{39}$$

Explicit formulas for the coefficient functions entering Eqs. (38b) are given in Appendix B together with some related comments. Evaluating these coefficients involves computing some products of Bessel spherical function and Wigner D functions and integrating these expressions over θ_k. Their numerical evaluation is relatively easy.

The coefficients with $j \neq j'$ describe angular momentum mixing. It can be shown that these terms go to zero in the absence of anisotropy, when $u=0$ and $n_e=1$.

The modes introduced in this subsection can be used to derive expansions for incident plane wave in the anisotropic medium [18]. In an isotropic material the corresponding ex-

pansions are given by Eqs. (5) and (8). In a uniformly anisotropic medium these expansions take an exactly analogous form:

$$\mathbf{E}_{jm}^{(inc)} = \alpha_{jm}^{(inc)}\,\mathbf{P}_{jm}^{(m)} - \frac{\mu}{n}\tilde{\alpha}_{jm}^{(inc)}\,\mathbf{P}_{jm}^{(e)},$$

$$\mathbf{H}_{jm}^{(inc)} = \tilde{\alpha}_{jm}^{(inc)}\,\mathbf{Q}_{jm}^{(m)} + \frac{n}{\mu}\alpha_{jm}^{(inc)}\,\mathbf{Q}_{jm}^{(e)}. \tag{40}$$

These equations can be compared to Eqs. (5). In the anisotropic case the spherical harmonics (4) are replaced by the ''quasispherical'' modes (37).

B. T matrix: uniform anisotropy

In Sec. IV A, computing the elements of T matrix for a radially anisotropic layer required the solution of a set of equations resulting from the boundary conditions (25). The only difference in other cases is that appropriate modes for the electromagnetic field inside the anisotropic layer must be used. For uniform anisotropy these modes are given by Eqs. (38). Mathematically, Eq. (26), which describe the fields in radially anisotropic layer, is replaced by the relation of the following form:

$$\begin{pmatrix} p_{jm}^{(m)} \\ q_{jm}^{(e)} \\ q_{jm}^{(m)} \\ p_{jm}^{(e)} \end{pmatrix} = \sum_{j' \geqslant |m|} \mathbf{R}^{jj';\,m}(r) \begin{pmatrix} \alpha_{j'm} \\ \beta_{j'm} \\ \tilde{\alpha}_{j'm} \\ \tilde{\beta}_{j'm} \end{pmatrix}. \tag{41}$$

The crucial difficulty in this case is that the algebraic structure of the equations is complicated by the presence of angular momentum mixing. Thus, by contrast with the radially anisotropic layer considered in Sec. IV A, we are now unable to derive expressions for the elements of the T matrix in closed form. The solution of this system of equations now requires numerical analysis.

In our subsequent calculations we put the magnetic permittivity equal to the unit and concentrate on the limiting case of a droplet, i.e., when the radius of the isotropic core of the scatterer, R_2, is negligible ($R_2 \to 0$). This case presents fewer technical difficulties than scattering by the annular layer. The crucial point is that the normal modes inside the droplet are all regular at the origin, and thus two types of modes that appear in the case of the annulus do not appear here. This reduces the number of variables in the problem by one half as compared to the scattering by a spherical annulus considered in Ref. [18].

So, the harmonics inside the droplet are

$$\mathbf{E}_{jm} = \alpha_{jm}^{(c)}\,\mathbf{P}_{jm}^{(m)} - n_o^{-1}\,\tilde{\alpha}_{jm}^{(c)}\,\mathbf{P}_{jm}^{(e)}, \tag{42a}$$

$$\mathbf{H}_{jm} = \tilde{\alpha}_{jm}^{(c)}\,\mathbf{Q}_{jm}^{(m)} + n_o\,\alpha_{jm}^{(c)}\,\mathbf{Q}_{jm}^{(e)}, \tag{42b}$$

where $\mathbf{P}_{jm}^{(\alpha)} = \mathbf{P}_{jm}^{(\alpha)}(\rho_o, \hat{\mathbf{r}})$, $\mathbf{Q}_{jm}^{(\alpha)} = \mathbf{Q}_{jm}^{(\alpha)}(\rho_o, \hat{\mathbf{r}})$, $\rho_o = m_o kr = m_o \rho$, $m_o \equiv n_o/n$ is the optical contrast, and $n_o = \sqrt{\epsilon_\perp} \equiv n_1$ is the ordinary wave refractive index. The modes $\mathbf{P}_{jm}^{(\alpha)}$ and $\mathbf{Q}_{jm}^{(\alpha)}$ have been given by Eqs. (23) for radial anisotropy and by Eqs. (37) for uniform anisotropy.

The continuity conditions at the outside of the droplet, $r = R_1$, can then be written in matrix notation as follows:

$$\sum_{j' \geqslant |m|} \mathbf{R}_1^{jj';\,m} \begin{pmatrix} \alpha_{j'm}^{(c)} \\ \tilde{\alpha}_{j'm}^{(c)} \end{pmatrix} = \mathbf{\Gamma}_1^j \begin{pmatrix} \alpha_{jm}^{(inc)} \\ \tilde{\alpha}_{jm}^{(inc)} \end{pmatrix} + \tilde{\mathbf{\Gamma}}_1^j \begin{pmatrix} \beta_{jm}^{(sca)} \\ \tilde{\beta}_{jm}^{(sca)} \end{pmatrix}, \tag{43}$$

$$\mathbf{\Gamma}^j(r) = \begin{pmatrix} j_j(\rho) & 0 \\ n[j_j(\rho)]' & 0 \\ 0 & j_j(\rho) \\ 0 & -n^{-1}[j_j(\rho)]' \end{pmatrix}, \tag{44}$$

where $\tilde{\mathbf{\Gamma}}^j$ is defined by the right-hand side of Eq. (44) with $j_j(\rho)$ replaced by $h_j^{(1)}(\rho)$; the index 1 indicates that matrix elements are calculated at the boundary of droplet, $r = R_1$.

In the case of a radially anisotropic droplet the matrix on the left-hand side of Eq. (43) is diagonal over angular momentum numbers [see Eq. (27)]. When the droplet is uniformly anisotropic, the matrix $\mathbf{R}^{jj';\,m}(r)$ is no longer diagonal. In this case it takes the form:

$$\mathbf{R}^{jj';\,m} = \begin{pmatrix} p_{jj';\,m}^{(m,m)} & -n_o^{-1}\,p_{jj';\,m}^{(m,e)} \\ n_o\,q_{jj';\,m}^{(e,e)} & q_{jj';\,m}^{(e,m)} \\ n_o\,q_{jj';\,m}^{(m,e)} & q_{jj';\,m}^{(m,m)} \\ p_{jj';\,m}^{(e,m)} & -n_o^{-1}\,p_{jj';\,m}^{(e,e)} \end{pmatrix}, \tag{45}$$

where the coefficients are functions of ρ_o and are given by Eqs. (B1)–(B8) in Appendix B.

The system (43) can be then simplified by multiplying both sides by the matrices

$$\frac{i}{\rho^2}\mathbf{H}^j(\rho) = \begin{pmatrix} [j_j]' & -n^{-1}\,j_j & 0 & 0 \\ 0 & 0 & n^{-1}\,[j_j]' & j_j \end{pmatrix} \tag{46}$$

and $\tilde{\mathbf{H}}^j(\rho)$ that can be obtained from $\mathbf{H}^j(\rho)$ by changing from j_j to $h_j^{(1)}$. Using the known expression for the Wronskian of the spherical Bessel functions [21], we derive a system equivalent to Eqs. (43) in the following form:

$$\boldsymbol{\alpha}_{jm}^{(inc)} = \sum_{j' \geqslant |m|} \mathbf{B}_{jj';\,m} \begin{pmatrix} \alpha_{j'm}^{(c)} \\ \tilde{\alpha}_{j'm}^{(c)} \end{pmatrix}, \tag{47a}$$

$$\boldsymbol{\beta}_{jm}^{(sca)} = \sum_{j' \geqslant |m|} \mathbf{A}_{jj';\,m} \begin{pmatrix} \alpha_{j'm}^{(c)} \\ \tilde{\alpha}_{j'm}^{(c)} \end{pmatrix}, \tag{47b}$$

where $\mathbf{A}_{jj';\,m} = -\mathbf{H}_1^j \cdot \mathbf{R}_1^{jj';\,m}$ and $\mathbf{B}_{jj';\,m} = \tilde{\mathbf{H}}_1^j \cdot \mathbf{R}_1^{jj';\,m}$.

From Eq. (47) we can immediately derive an expression for the T matrix:

$$\mathbf{T}_{jj';\,m} = [\mathbf{A} \cdot \mathbf{B}^{-1}]_{jj';\,m}. \tag{48}$$

For radial anisotropy all the matrices on the right-hand sides of Eqs. (47) are diagonal. So, it is easy to write down the result for the T matrix $\mathbf{T}_{jj';\,m}=\delta_{jj'}\mathbf{T}_j$:

$$T_j^{11}=-\frac{[j_j(\rho_o)]_1[j_j(\rho)]_1'-m_o[j_j(\rho_o)]_1'[j_j(\rho)]_1}{[j_j(\rho_o)]_1[h_j^{(1)}(\rho)]_1'-m_o[j_j(\rho_o)]_1'[h_j^{(1)}(\rho)]_1}, \tag{49a}$$

$$T_j^{22}=-\frac{m_o[j_{\tilde{j}}(\rho_o)]_1[j_j(\rho)]_1'-[j_{\tilde{j}}(\rho_o)]_1'[j_j(\rho)]_1}{m_o[j_{\tilde{j}}(\rho_o)]_1[h_j^{(1)}(\rho)]_1'-[j_{\tilde{j}}(\rho_o)]_1'[h_j^{(1)}(\rho)]_1}. \tag{49b}$$

These formulas bear close resemblance to the well known Mie expressions [17].

VI. NUMERICAL RESULTS

From a mathematical point of view, the radial and uniform anisotropies present interesting but contrasting features. Here we draw the reader's attention to some of the most striking of these.

Clearly, the difference in symmetry causes the most crucial differences in the light scattering. Radially anisotropic layer presents an isotropic face to the world, to the extent that the scattering properties are independent of the direction of the incident wave. Here the scattering material is locally optically anisotropic, but because of the way that the anisotropy is arranged, the scatterer itself is spherically symmetric and remains a globally optically isotropic object. The result is that there is no angular momentum mixing and the scattering efficiency does not depend on the angle of incidence and the polarization of incoming wave.

In the case of uniform anisotropy, this is no longer true. In this case the scattering geometry is shown in Fig. 1(b) and we shall discuss quantitative results for uniformly anisotropic droplets later in this section.

A. Radially anisotropic layer and effective isotropic scatterer

We have seen above that the scattering from radially anisotropic layer shares some features of isotropic scatterers, although we do have to introduce the new normal mode structure 22 within the anisotropic layer. It is our purpose here to show briefly that the anisotropy effects can be important, even for this relatively simple case.

As an example, we compare scattering by a radially anisotropic layer and an isotropic layer of the same dimensions, chosen in some sense to be the best guess to an equivalent isotropic scatterer. Specifically, we consider scattering by a scatterer with a radially anisotropic layer as discussed in Sec. II, with the $\epsilon_\perp$ within the layer matching ϵ in the core and outside the scatterer, and anisotropy coefficient u inside the layer. The equivalent effective scatterer has the same dimensions, possesses an isotropic layer of refractive index n_{eff}, so that ϵ_{eff} is the dielectric constant and $m_{\text{eff}}=n_{\text{eff}}/n$ is the optical contrast. The refractive index n_{eff} is chosen so as to match scattering efficiencies of the anisotropic layer and of the effective scatterer.

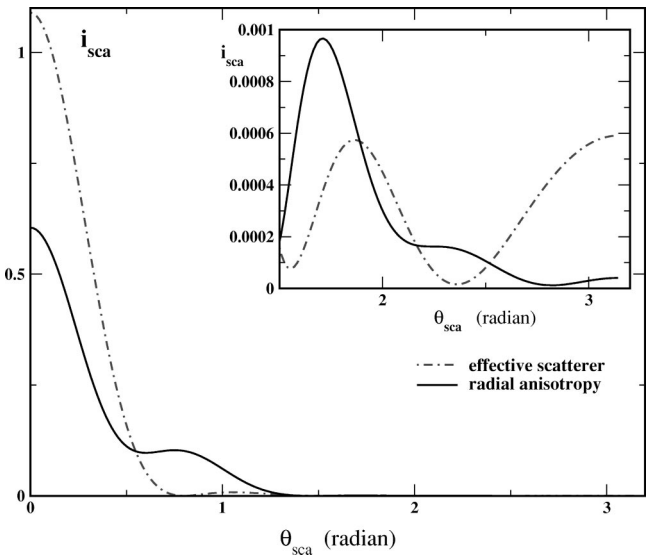

FIG. 2. Scattered intensity [see Eq. (20)] versus the scattering angle at $kR_2=1.5, kd=4.0$, and $u_1=0.25$ for (a) effective isotropic scatterer with $m_{\text{eff}}\approx 1.051\,27$ ($Q_{\text{eff}}=0.143\,91$) and (b) radially anisotropic layer, $\hat{\mathbf{n}}=\hat{\mathbf{r}}$($Q_{Mie}=0.1439$). Insert at the upper right corner enlarges the backscattering tail.

We compare the angular dependence of the scattering 20 and the depolarization factors 21 in the two cases. The aggregate scattering is the same, by definition. But disaggregated, we get different contributions, both when looking at angles and when looking at polarization shifts. In Fig. 2 we compare the angular dependence of the intensities. In the case we have considered, the effective scatterer gives a much more forward scattering signature, and the relatively tiny backward scattering contribution has a very different angular structure. Likewise, we see from Fig. 3 that the depolarization factor (21) as a function of the scattering angle θ_{sca} is

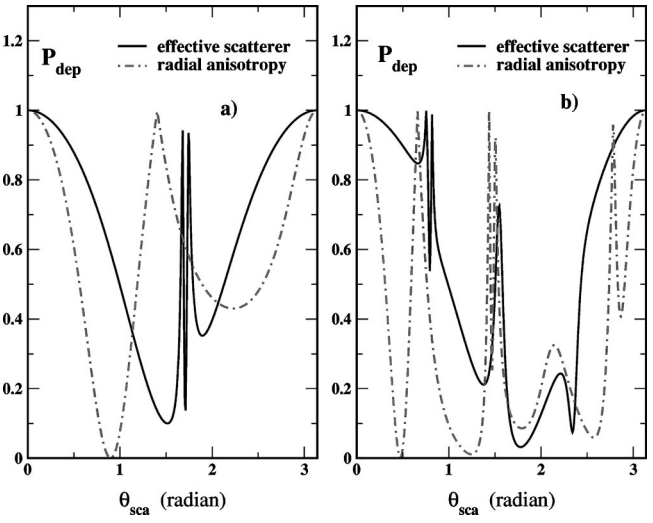

FIG. 3. Depolarization factor [see Eq. (21)] versus the scattering angle for both the radially anisotropic layer and its effective isotropic scatterer at $kR_2=1.5, u_1=0.25$ and (a) $kd=1.0$ ($m_{\text{eff}}\approx 1.045\,12, Q_{\text{eff}}=0.010\,724, Q_{rad}=0.010\,729$), (b) $kd=4.0$ ($m_{\text{eff}}\approx 1.05\,127, Q_{\text{eff}}=0.143,91, Q_{rad}=0.1439$).

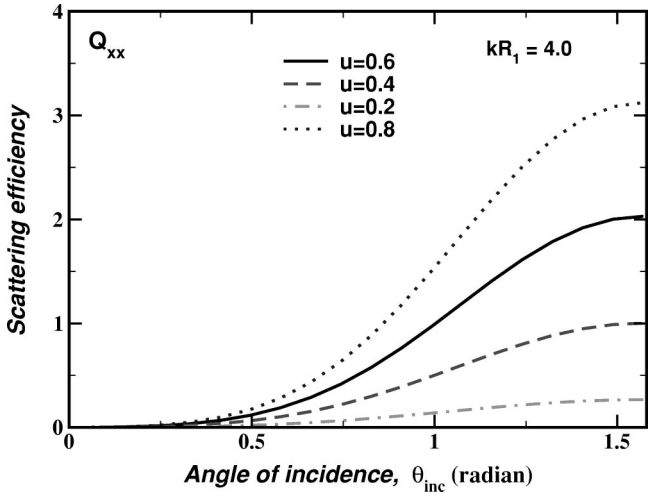

FIG. 4. Scattering efficiency of uniformly anisotropic droplet as a function of the angle of incidence (the angle between the incident wave and the optical axis) at various values of the anisotropy parameter, $u=(\epsilon_{\parallel}-\epsilon_{\perp})/\epsilon_{\perp}$, with $kR_1=4.0$ and $n=n_o$.

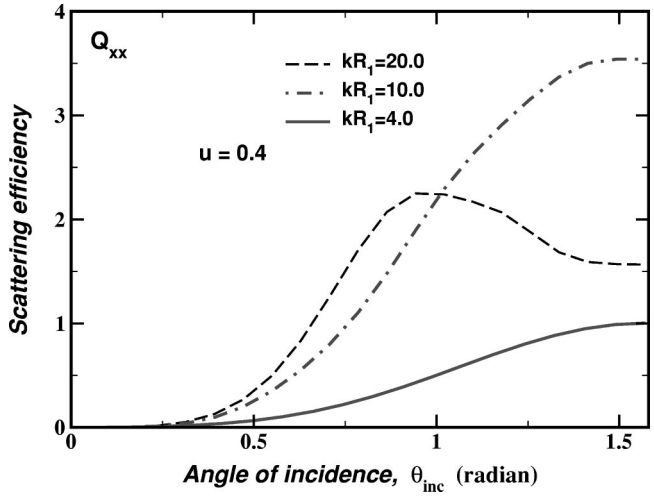

FIG. 5. Dependence of the scattering efficiency on the angle of incidence for uniformly anisotropic droplet at various values of the size parameter and $u=0.4$. The refractive indices n and n_o are matched.

also very sensitive to the presence of anisotropy.

Given these relatively large effects for what might be thought of as minor anisotropy, there is every reason to suppose that the influence of a uniform anisotropy will be even more profound.

B. Radially and uniformly anisotropic droplets

In this section we present numerical results for the scattering efficiency defined by Eqs. (15) and (16). We are primarily interested in anisotropy-induced scattering. In order to concentrate on this test case, we consider the case when the refractive indices n and n_o are equal. We shall present a more comprehensive analysis of all possible cases, including the results for the angular distribution of the scattered waves, elsewhere. We begin with brief comments on numerical procedure and then proceed with the description of the calculated dependencies.

It is rather straightforward to perform computations for radially anisotropic droplets. The expressions for the elements of T matrix are known and given by Eqs. (49a) and (49b). We can thus evaluate the scattering efficiency by explicitly computing the sum in the expression (18).

For uniformly anisotropic droplets T matrix can only be computed numerically by solving the system of equations (47) [32]. In this case we have rather strong dependence of the scattering efficiency on both the angle of incidence, which is the angle between the direction of incidence and the optical axis [see Fig. 1(b)], and the polarization of the incoming wave. In particular, when the refractive indices are matched, $n=n_o$, it is expected that the scatterer does not change the y component of the incident wave, which simply transforms into the ordinary wave inside the droplet without being affected by the scattering process. The algebraic interpretation of this fact is that the amplitudes of the scattered wave $\beta_{jm;y}^{(sca)}$ and $\tilde{\beta}_{jm;y}^{(sca)}$ are equal to zero and the quantity of interest is Q_{xx}, which is the only nonvanishing component of the scattering efficiency tensor (16). However, it is not straightforward to see that the system (47) is consistent with this conclusion. We show this in Appendix C. Some highlights of the results are presented below.

The dependence of the scattering efficiency on the angle of incidence is shown in Fig. 4. If the size parameter, kR_1, is not very large, the scattering efficiency Q_{xx} is a monotonically increasing function of the angle of incidence, θ_{inc}, in the region from 0 to $\pi/2$. By symmetry $Q_{xx}(\theta_{inc})=Q_{xx}(\pi/2-\theta_{inc})$, and so the scattering efficiency decreases in the range from $\pi/2$ to π.

In Fig. 5 we show what happens for shorter wavelength and thus higher values of kR_1. Now, for relatively large values of the size parameter, the cross-section dependence on the angle of incidence is no longer monotonic. For example, at $kR_1=20.0$, the angle at which the scattering efficiency Q_{xx} reaches its maximum value is no longer at $\pi/2$.

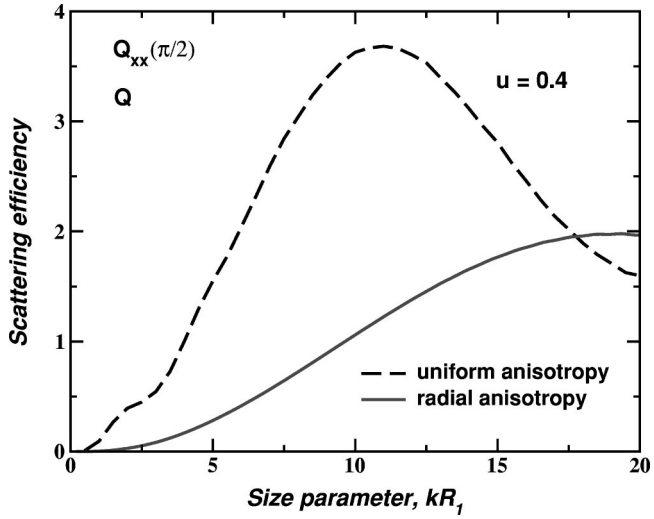

FIG. 6. Scattering efficiencies of radially and uniformly anisotropic droplets versus the size parameter at $u=0.4$, $\theta_{inc}=\pi/2$, and $n=n_o$.

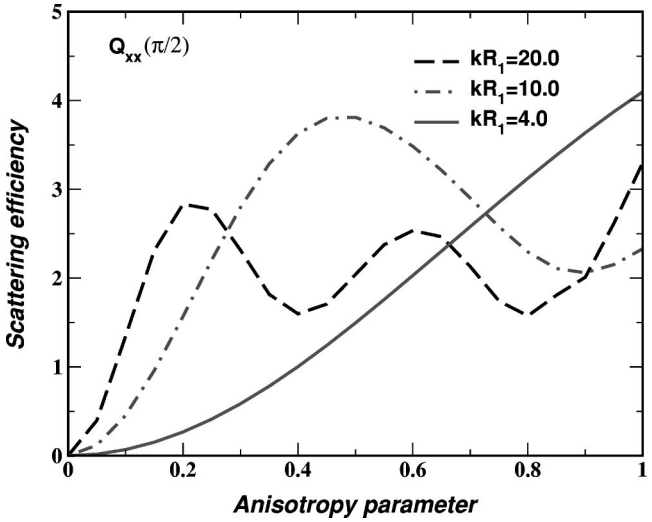

FIG. 7. Scattering efficiencies of uniformly anisotropic droplets versus the anisotropy parameter at various values of the size parameter for $\theta_{inc}=\pi/2$ and $n=n_o$.

Figure 6 shows the scattering efficiencies $Q_{xx}(\pi/2)$ (for uniform anisotropy) and Q (for radial anisotropy) versus the size parameter. The scattering efficiency of uniformly anisotropic droplet has a pronounced peak located at about $kR_1 \approx 10.0$ and exhibits strongly nonmonotonic behavior. By contrast, the corresponding dependence for the radially anisotropic droplet is monotonically increasing. In this case the first maximum is reached at $kR_1 \approx 20.0$, outside the range of kR_1 shown in Fig. 6.

The scattering efficiencies as a function of the anisotropy parameter, $0 \leqslant u \leqslant 1$, at different values of the size parameter are plotted in Fig. 7 and Fig. 8 for the cases of radial and uniform anisotropies, respectively. In both cases an increase in the size parameter leads to the appearance of peaks in this range of u. As compared to radially anisotropic scatterers, the uniformly anisotropic droplets seem to be more sensitive to changes both in the size and in the anisotropy parameters.

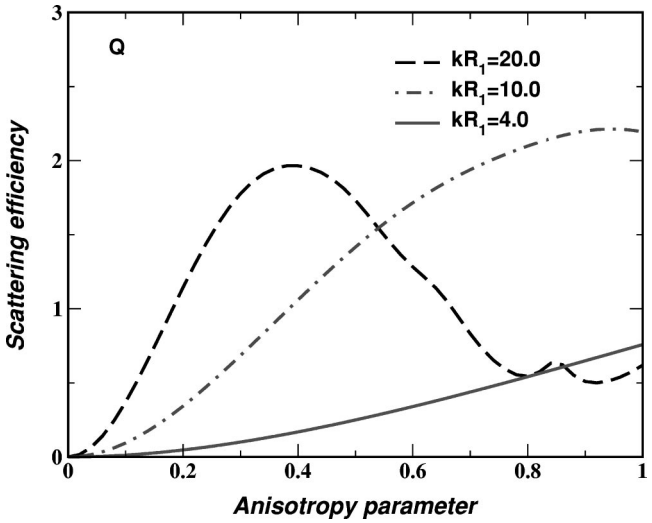

FIG. 8. Dependence of the scattering efficiency on the anisotropy parameter for radially anisotropic droplets at various values of the size parameter and $n=n_o$.

VII. DISCUSSION AND CONCLUSIONS

In this paper we have developed a *T*-matrix approach that can describe light scattering by spherical scatterers containing optically anisotropic material arranged in an annular layer. We have confined our discussion to the two cases, which we have called, using natural language, radially and uniformly anisotropic systems. Just as in the related case when the scatterer itself is anisotropic, but the scattering material is optically isotropic, the presence of optical anisotropy affects the algebraic structure that underlies the *T* matrix theory.

In the case of the uniform anisotropy the light-scattering problem is not exactly soluble. The key point is that the *exact solutions* for uniformly anisotropic medium are known as plane waves, whereas the spherical shape of the particle requires using some kind of spherical modes.

We have found that, by choosing the appropriate basis in $\hat{\mathbf{k}}$ space, we can define ''quasispherical'' normal modes. These modes are *exact solutions* of Maxwell's equations and as such mix different angular momentum. However, in the limit of zero anisotropy, these modes tend to familiar spherical modes. More importantly, these quasispherical modes turn out to be relatively easily accessible computationally. In order to show this, we have described some of the numerical results calculated using the *T*-matrix theory presented in this paper. In particular, we have studied the scattering efficiency of radially and uniformly anisotropic droplets in which the ordinary refractive index matches the refractive index of the material surrounding them.

The assumption in which the ordinary refractive index of the droplet matches the isotropic dielectric constant in the surrounding medium is not taken in order to simplify the numerical treatment. Rather in this paper we wish to study the light-scattering properties that can be solely attributed to the *anisotropic* part of the dielectric tensor. Thus we have the anisotropy effects separated out to concentrate on differences between isotropic and anisotropic optical axis distributions.

The graphs plotted in Figs. 6–8 indicate that uniformly anisotropic droplets are more sensitive to changes in the wavelength and anisotropy parameters than are radially anisotropic droplets. Our results are also consistent with results of previous studies [8,14] that the internal spatial distribution of the optical axis is a factor that strongly affects light scattering from anisotropic scatterers.

The results of this work can be regarded as the first step towards more comprehensive study of light scattering by anisotropic scatterers. We have demonstrated that the *T*-matrix approach developed in this paper can be used in an efficient numerical treatment of the scattering problem. It is thus reasonable to expect that further progress can be made by applying this theory to more complex problems.

One such problem is the light-scattering problem for a Faraday-active sphere. This problem has been treated using perturbation theory in Ref. [27] to explain the origin of magnetotransverse light diffusion known as the ''photonic Hall effect'' [28,29].

We now try to place this problem in a more general physical context. We were first motivated by the technological problem of describing light transmission through media with liquid crystalline inclusions, and the inverse problem in which the matrix is liquid crystalline but the scatterers are isotropic. There is considerable current interest in such materials for optical applications and displays. The complete problem of light transmission through such materials not only involves the single scattering processes discussed in this paper, but also more general multiple scattering processes.

The *T*-matrix formalism is a natural language within which to discuss such problems. Beginning with single scattering theories of the type discussed in this paper, one can in principle construct an effective medium theory using, for example, the coherent potential approximation (CPA) or coated CPA [30,31]. These theories determine effective optical characteristics of the medium from the condition that the scattering cross section is minimal or equal to zero on average. Since this requires averaging over director orientations, it is important to use basis functions with well defined transformation properties under rotations.

ACKNOWLEDGMENTS

We acknowledge support from INTAS under Grant No. 99-0312. A.K. thanks the Faculty of Mathematical Studies in the University of Southampton.

APPENDIX A: VECTOR SPHERICAL HARMONICS AND RAYLEIGH EXPANSIONS FOR VECTOR PLANE WAVES

In this appendix we introduce notations and definitions used throughout the paper. In addition, we express the vector spherical harmonics in terms of Wigner *D* functions and deduce Rayleigh expansions for vector plane waves.

Let us define the vectors

$$\mathbf{e}_{\pm 1}(\hat{\mathbf{r}}) = \mp(\hat{\boldsymbol{\vartheta}} \pm i\hat{\boldsymbol{\varphi}})/\sqrt{2} \equiv \mp[\mathbf{e}_x(\hat{\mathbf{r}}) \pm i\,\mathbf{e}_y(\hat{\mathbf{r}})]/\sqrt{2},$$

$$\mathbf{e}_0(\hat{\mathbf{r}}) \equiv \hat{\mathbf{r}}, \tag{A1}$$

where $\hat{\boldsymbol{\varphi}} = (-\sin\phi, \cos\phi, 0)$, $\hat{\boldsymbol{\vartheta}} = (\cos\theta\cos\phi, \cos\theta\sin\phi, -\sin\theta)$ are the unit vectors tangential to the sphere; ϕ and θ are Euler angles of the unit vector $\hat{\mathbf{r}}$. These vectors can be expressed in terms of the vectors of spherical basis, $\mathbf{e}_0 \equiv \hat{\mathbf{z}}$, $\mathbf{e}_{\pm 1} = \mp(\hat{\mathbf{x}} \pm i\hat{\mathbf{y}})/\sqrt{2}$, ($\hat{\mathbf{x}}$, $\hat{\mathbf{y}}$, and $\hat{\mathbf{z}}$ are the unit vectors directed along the corresponding coordinate axes) as follows:

$$\mathbf{e}_\nu(\hat{\mathbf{r}}) = \sum_{\mu=-1}^{1} D^1_{\mu\nu}(\hat{\mathbf{r}})\mathbf{e}_\mu, \tag{A2}$$

where $D^j_{\mu\nu}(\hat{\mathbf{r}}) \equiv D^j_{\mu\nu}(\phi,\theta) = e^{-i\mu\phi} d^j_{\mu\nu}(\theta)$ is the Wigner *D* function [20,22].

The vector spherical functions $\mathbf{Y}^{(\alpha)}_{jm}$ from Eqs. (2) are expressed in terms of the vector spherical harmonics $\mathbf{Y}_{ljm}$ [20] defined by

$$\mathbf{Y}_{ljm} = \sum_{\nu=-1}^{1} C^{l\,1\,j}_{m-\nu\,\nu\,m} Y_{l\,m-\nu} \otimes \mathbf{e}_\nu, \tag{A3}$$

where $Y_{lm} = \sqrt{(2l+1)/(4\pi)} D^{l}_{m\,0}{}^{*}$ is the spherical function [21] and $C^{j+\delta\,1\,j}_{m-\nu\,\nu m}$ denotes the Clebsch-Gordon (Wigner) coefficient,

$$\mathbf{Y}^{(m)}_{jm} = \mathbf{Y}_{j\,j\,m}, \tag{A4a}$$

$$\mathbf{Y}^{(e)}_{jm} = s_j \mathbf{Y}_{j+1\,j\,m} + c_j \mathbf{Y}_{j-1\,jm}, \tag{A4b}$$

$$\mathbf{Y}^{(o)}_{jm} = -c_j \mathbf{Y}_{j+1\,jm} + s_j \mathbf{Y}_{j-1\,jm}, \tag{A4c}$$

$$s_j \equiv \left[\frac{j}{2j+1}\right]^{1/2}, \quad c_j \equiv \left[\frac{j+1}{2j+1}\right]^{1/2}.$$

Eqs. (A2), (A3), and the equality [20]

$$C^{j_1 j_2 j}_{k_1 k_2 k} D^j_{mk} = \sum_{m_1 m_2} C^{j_1\,j_2\,j}_{m_1 m_2 m} D^{j_1}_{m_1 k_1} D^{j_2}_{m_2 k_2} \tag{A5}$$

give

$$[\mathbf{Y}^*_{ljm}(\hat{\mathbf{r}}) \cdot \mathbf{e}_\nu(\hat{\mathbf{r}})] = N_j C^{lj}_\nu D^j_{m\nu}(\hat{\mathbf{r}}), \tag{A6}$$

where $N_j = \sqrt{(2j+1)/4\pi}$ and $C^{lj}_\nu \equiv [(2l+1)/(2j+1)]^{1/2} C^{l\,1\,j}_{0\,\nu\,\nu}$, so that the nonvanishing values of C^{lj}_ν are

$$\sqrt{2}\, C^{jj}_\nu = -\nu, \qquad \sqrt{2}\, C^{j-1\,j}_{\pm 1} = -C^{j+1\,j}_0 = c_j,$$

$$\sqrt{2}\, C^{j+1\,j}_{\pm 1} = C^{j-1\,j}_0 = s_j. \tag{A7}$$

From Eqs. (A4), (A6), and (A7) we express the vector spherical harmonics in terms of the Wigner *D* functions as follows:

$$\mathbf{Y}^{(e,m)}_{jm}(\hat{\mathbf{r}}) = N_j\{D^{j}_{m,-1}{}^{*}(\hat{\mathbf{r}})\mathbf{e}_{-1}(\hat{\mathbf{r}}) \pm D^{j}_{m,1}{}^{*}(\hat{\mathbf{r}})\mathbf{e}_{+1}(\hat{\mathbf{r}})\}/\sqrt{2}, \tag{A8a}$$

$$\mathbf{Y}^{(o)}_{jm}(\hat{\mathbf{r}}) = N_j\, D^{j}_{m,0}{}^{*}(\hat{\mathbf{r}})\mathbf{e}_0(\hat{\mathbf{r}}). \tag{A8b}$$

Note that the *D* functions meet the following orthogonality relations [20,22]:

$$\langle D^{j}_{m\nu}{}^{*}(\hat{\mathbf{r}}) D^{j'}_{m'\nu}(\hat{\mathbf{r}})\rangle_{\hat{\mathbf{r}}} = \frac{4\pi}{2j+1}\delta_{jj'}\delta_{mm'}, \tag{A9}$$

where $\langle f\rangle_{\hat{\mathbf{r}}} \equiv \int_0^{2\pi} d\phi \int_0^{\pi} \sin\theta d\theta f$. The orthogonality condition (A9) and Eqs. (A8a) and (A8b) show that a set of vector spherical harmonics is orthonormal:

$$\langle \mathbf{Y}^{(\alpha)}_{jm}{}^{*}(\hat{\mathbf{r}}) \cdot \mathbf{Y}^{(\beta)}_{j'm'}(\hat{\mathbf{r}})\rangle_{\hat{\mathbf{r}}} = \delta_{\alpha\beta}\,\delta_{jj'}\,\delta_{mm'}. \tag{A10}$$

We can now comment on the vector version of the well known Rayleigh expansion (see, for example, Ref. [12]):

$$e^{i\rho(\hat{\mathbf{k}}\cdot\hat{\mathbf{r}})} = 4\pi \sum_{l=0}^{\infty} \sum_{m=-l}^{l} i^l j_l(\rho)\, Y_{lm}(\hat{\mathbf{r}}) Y^*_{lm}(\hat{\mathbf{k}}). \tag{A11}$$

Let us consider a plane wave with the wave vector $\mathbf{k} \equiv k\hat{\mathbf{k}}$ and the polarization vector $\mathbf{E}$ defined by its components, E_ν, in the basis $\mathbf{e}_\nu(\hat{\mathbf{k}})$ [see Eq. (A2)].

From Eq. (A11), definition of the vector spherical functions (A4), and the equality (A5) it is not difficult to derive the following relation:

$$\mathbf{e}_\nu(\hat{\mathbf{k}})e^{i(\mathbf{k}\cdot\mathbf{r})}=\sum_{j,m}\,[2\pi(2j+1)]^{1/2}D^j_{m\nu}(\hat{\mathbf{k}}) \times\left[\sum_l\, i^l j_l(\rho)C^{lj}_\nu\,\mathbf{Y}_{ljm}(\hat{\mathbf{r}})\right], \qquad \text{(A12)}$$

where $D^j_{\mu\nu}(\hat{\mathbf{k}})\equiv D^j_{\mu\nu}(\phi_k,\theta_k)$, C^{lj}_ν is defined in Eq. (A7) and ϕ_k, θ_k are the azimuthal and polar angles of the unit vector $\hat{\mathbf{k}}$. The sum in square brackets on the right-hand side of Eq. (A12) can be simplified by using Eq. (A7) and the recursion relations for spherical Bessel functions [21]. The final result for transverse waves can be written in the following form:

$$\mathbf{e}_x(\hat{\mathbf{k}})\exp(i\,\mathbf{k}\cdot\mathbf{r})=\sum_{j,m}\,\alpha_j[D^{(y)}_{jm}(\hat{\mathbf{k}})\mathbf{M}^{(m)}_{jm}(\rho,\hat{\mathbf{r}}) - iD^{(x)}_{jm}(\hat{\mathbf{k}})\mathbf{M}^{(e)}_{jm}(\rho,\hat{\mathbf{r}})], \qquad \text{(A13a)}$$

$$\mathbf{e}_y(\hat{\mathbf{k}})\exp(i\,\mathbf{k}\cdot\mathbf{r})=\sum_{j,m}\,\alpha_j[iD^{(x)}_{jm}(\hat{\mathbf{k}})\mathbf{M}^{(m)}_{jm}(\rho,\hat{\mathbf{r}}) + D^{(y)}_{jm}(\hat{\mathbf{k}})\mathbf{M}^{(e)}_{jm}(\rho,\hat{\mathbf{r}})], \qquad \text{(A13b)}$$

where $\alpha_j\equiv i^j[\pi(2j+1)]^{1/2}$, the modes $\mathbf{M}^{(m)}_{jm}$, $\mathbf{M}^{(e)}_{jm}$ are defined by Eq. (4a) and the functions $D^{(x)}_{jm}$, $D^{(y)}_{jm}$ are expressed in terms of Wigner D functions in Eq. (32).

In conclusion, we shall write the formulas for the matrix elements of the plane wave with polarization vector directed along the z axis: $\langle \mathbf{Y}^{(\alpha)}_{jm}{}^*\cdot\hat{\mathbf{z}}\exp(i\,\mathbf{k}\cdot\mathbf{r})\rangle_{\hat{\mathbf{r}}}$. The result is as follows:

$$\langle \mathbf{Y}^{(m)}_{jm}{}^*\cdot\hat{\mathbf{z}}\exp(i\,\mathbf{k}\cdot\mathbf{r})\rangle_{\hat{\mathbf{r}}} =i^j[4\pi(2j+1)]^{1/2}C^{j\,1\,j}_{m\,0\,m}D^j_{m0}(\hat{\mathbf{k}})j_j(\rho), \qquad \text{(A14a)}$$

$$\langle \mathbf{Y}^{(e)}_{jm}{}^*\cdot\hat{\mathbf{z}}\exp(i\,\mathbf{k}\cdot\mathbf{r})\rangle_{\hat{\mathbf{r}}} =i^{j+1}[4\pi]^{1/2}[(2j+3)^{1/2}s_jC^{j+1\,1\,j}_{m\,0\,m}D^{j+1}_{m0}(\hat{\mathbf{k}})\,j_{j+1}(\rho) -(2j-1)^{1/2}c_jC^{j-1\,1\,j}_{m\,0\,m}D^{j-1}_{m0}(\hat{\mathbf{k}})j_{j-1}(\rho)], \qquad \text{(A14b)}$$

$$\langle \mathbf{Y}^{(o)}_{jm}{}^*\cdot\hat{\mathbf{z}}\exp(i\,\mathbf{k}\cdot\mathbf{r})\rangle_{\hat{\mathbf{r}}} =i^{j+1}[4\pi]^{1/2}[(2j+3)^{1/2}c_jC^{j+1\,1\,j}_{m\,0\,m}D^{j+1}_{m0}(\hat{\mathbf{k}})j_{j+1}(\rho) +(2j-1)^{1/2}s_jC^{j-1\,1\,j}_{m\,0\,m}D^{j-1}_{m0}(\hat{\mathbf{k}})j_{j-1}(\rho)]. \qquad \text{(A14c)}$$

APPENDIX B: COEFFICIENT FUNCTIONS

By definition, the coefficient functions that enter the expansions (38) are the matrix elements (39). In order to deduce the corresponding formulas we need to substitute the expansions for plane waves Eqs. (A13) into Eqs. (37) and use the matrix elements for the plane wave polarized along the z axis given by Eqs. (A14a)–(A14c).

The resulting expressions for the matrix elements that correspond to transverse components of the wave functions (37) are

$$p^{(m,m)}_{jj';m}(\rho)=N_{jj'}\langle d^{(y;y)}_{j'j;m}j_j(\rho_e)+d^{(x;x)}_{j'j;m}j_j(\rho)\rangle_{\theta_k}+\Delta p^{(m,m)}_{jj';m}(\rho), \qquad \text{(B1)}$$

$$p^{(m,e)}_{jj';m}(\rho)=i\,N_{jj'}\langle d^{(x;y)}_{j'j;m}j_j(\rho_e)+d^{(y;x)}_{j'j;m}j_j(\rho)\rangle_{\theta_k}+\Delta p^{(m,e)}_{jj';m}(\rho), \qquad \text{(B2)}$$

$$p^{(e,m)}_{jj';m}(\rho)=-i\,N_{jj'}\langle d^{(y;x)}_{j'j;m}Dj_j(\rho_e)+d^{(x;y)}_{j'j;m}Dj_j(\rho)\rangle_{\theta_k} +\Delta p^{(m,e)}_{jj';m}(\rho), \qquad \text{(B3)}$$

$$p^{(e,e)}_{jj';m}(\rho)=N_{jj'}\langle d^{(x;x)}_{j'j;m}Dj_j(\rho_e)+d^{(y;y)}_{j'j;m}Dj_j(\rho)\rangle_{\theta_k} +\Delta p^{(e,e)}_{jj';m}(\rho), \qquad \text{(B4)}$$

$$q^{(m,m)}_{jj';m}(\rho)=N_{jj'}\langle d^{(x;x)}_{j'j;m}j_j(\rho_e)n_e^{-1}+d^{(y;y)}_{j'j;m}j_j(\rho)\rangle_{\theta_k}, \qquad \text{(B5)}$$

$$q^{(m,e)}_{jj';m}(\rho)=i\,N_{jj'}\langle d^{(y;x)}_{j'j;m}j_j(\rho_e)n_e^{-1}+d^{(x;y)}_{j'j;m}j_j(\rho)\rangle_{\theta_k}, \qquad \text{(B6)}$$

$$q^{(e,m)}_{jj';m}(\rho)=-i\,N_{jj'}\langle d^{(x;y)}_{j'j;m}Dj_j(\rho_e)n_e^{-1}+d^{(y;x)}_{j'j;m}Dj_j(\rho)\rangle_{\theta_k}, \qquad \text{(B7)}$$

$$q^{(e,e)}_{jj';m}(\rho)=i\,N_{jj'}\langle d^{(y;y)}_{j'j;m}Dj_j(\rho_e)n_e^{-1}+d^{(x;x)}_{j'j;m}Dj_j(\rho)\rangle_{\theta_k}, \qquad \text{(B8)}$$

where $N_{jj'}\equiv i^{j'-j}/8[(2j+1)(2j'+1)]^{1/2}$ and $d^{(\alpha;\beta)}_{jj';m}\equiv d^{(\alpha)}_{jm}(\theta_k)d^{(\beta)}_{j'm}(\theta_k)$, $\alpha,\beta\in\{x,y,z\}$. The terms $\Delta p^{(\alpha,\beta)}_{jj';m}(\rho)$ are given by

$$\Delta p^{(m,m)}_{jj';m}(\rho)=N_{jj'}\frac{2m}{\sqrt{j(j+1)}}r^{(z,x)}_{jj';m}(\rho), \qquad \text{(B9)}$$

$$\Delta p^{(m,e)}_{jj';m}(\rho)=N_{jj'}\frac{2m}{\sqrt{j(j+1)}}r^{(z,y)}_{jj';m}(\rho), \qquad \text{(B10)}$$

$$\Delta p^{(e,m)}_{jj';m}(\rho)=N_{jj'}\frac{-2\,i}{2j+1}\{\{j[(j+1)^2-m^2]/(j+1)\}^{1/2}\times r^{(z,y)}_{j+1\,j';m}(\rho)-[(j+1)(j^2-m^2)/j]^{1/2}\times r^{(z,y)}_{j-1\,j';m}(\rho)\}, \tag{B11}$$

$$\Delta p^{(e,e)}_{jj';m}(\rho)=N_{jj'}\frac{2}{2j+1}\{\{j[(j+1)^2-m^2]/(j+1)\}^{1/2}\times r^{(z,x)}_{j+1\,j';m}(\rho)-[(j+1)(j^2-m^2)/j]^{1/2}\times r^{(z,x)}_{j-1\,j';m}(\rho)\}, \tag{B12}$$

where

$$r^{(z,\alpha)}_{j\,j';m}(\rho)=\frac{u}{u+1}\langle d^{(\alpha;z)}_{j'j;m}(\theta_k)j_j(\rho_e)\sin\theta_k\rangle_{\theta_k}. \tag{B13}$$

Expressions for $\tilde{p}^{(\alpha,\beta)}_{jj';m}(\rho)$ and $\tilde{q}^{(\alpha,\beta)}_{jj';m}(\rho)$ can be derived from Eqs. (B1)–(B13) by replacing spherical Bessel functions of the first kind $j_j(x)$ with spherical Bessel functions of the third kind $h^{(1)}_j(x)$.

Using the orthogonality condition (A9) it can be shown that the coefficient functions $p^{(\alpha,\beta)}_{jj';m}$ and $q^{(\alpha,\beta)}_{jj';m}$ are diagonal, $\propto\delta_{\alpha\beta}\delta_{jj'}$, in the limit of weak anisotropy, $u\to 0$.

APPENDIX C

In this appendix we show mathematically, using our formalism, the physically obvious result that if the ordinary refractive index of a droplet matches that of the scattering medium, then there will be no scattering of the polarization component out of the plane of the incident wave and the uniform anisotropy in the droplet. In order to do this, we first extend algebraic relations that follow from Eqs. (40). These equations give the expansion of plane wave propagating in a uniformly anisotropic medium. We can rewrite them for the plane wave inside the droplet:

$$\sum_{j'm'}[\alpha^{(inc)}_{j'm'}\mathbf{P}^{(m)}_{j'm'}(\rho_o,\hat{\mathbf{r}})-n_o^{-1}\tilde{\alpha}^{(inc)}_{j'm'}\mathbf{P}^{(e)}_{j'm'}(\rho_o,\hat{\mathbf{r}})]=\exp(i\rho_e\hat{\mathbf{k}}_{inc}\cdot\hat{\mathbf{r}})E_x(\hat{\mathbf{k}}_{inc})\left[\mathbf{e}_x(\hat{\mathbf{k}}_{inc})+\frac{u\sin\theta_{inc}}{1+u}\hat{\mathbf{z}}\right]+\exp(i\rho_o\hat{\mathbf{k}}_{inc}\cdot\hat{\mathbf{r}})E_y(\hat{\mathbf{k}}_{inc})\mathbf{e}_y(\hat{\mathbf{k}}_{inc}), \tag{C1}$$

$$\sum_{j'm'}[\tilde{\alpha}^{(inc)}_{j'm}\mathbf{Q}^{(m)}_{j'm'}(\rho_o,\hat{\mathbf{r}})+n_o\alpha^{(inc)}_{j'm'}\mathbf{Q}^{(e)}_{j'm'}(\rho_o,\hat{\mathbf{r}})]=n_o[\exp(i\rho_e\hat{\mathbf{k}}_{inc}\cdot\hat{\mathbf{r}})m_e^{-1}E_x(\hat{\mathbf{k}}_{inc})\mathbf{e}_y(\hat{\mathbf{k}}_{inc})-\exp(i\rho_o\hat{\mathbf{k}}_{inc}\cdot\hat{\mathbf{r}})E_y(\hat{\mathbf{k}}_{inc})\mathbf{e}_x(\hat{\mathbf{k}}_{inc})], \tag{C2}$$

where $m_e=\sqrt{(1+u)/(1+u\cos^2\theta_{inc})}$ and $\rho_e=m_e\rho_o$. The coefficients $\alpha^{(inc)}_{jm}$ and $\tilde{\alpha}^{(inc)}_{jm}$ are defined by Eqs. (8) where the factor μ/n is changed to $1/n_o$.

We can now combine the relations that come from definitions of the coefficient functions [see Eq. (39)]

$$\sum_{j'\geqslant|m|}[p^{(\alpha,m)}_{jj';m}(\rho_o)\alpha^{(inc)}_{j'm}-n_o^{-1}p^{(\alpha,e)}_{jj';m}(\rho_o)\tilde{\alpha}^{(inc)}_{j'm}]=\left\langle\mathbf{Y}^{(\alpha)}_{jm}{}^*(\hat{\mathbf{r}})\cdot\sum_{j'm'}[\alpha^{(inc)}_{j'm'}\mathbf{P}^{(m)}_{j'm'}(\rho_o,\hat{\mathbf{r}})-n_o^{-1}\tilde{\alpha}^{(inc)}_{j'm'}\mathbf{P}^{(e)}_{j'm'}(\rho_o,\hat{\mathbf{r}})]\right\rangle_{\hat{\mathbf{r}}}, \tag{C3}$$

$$\sum_{j'\geqslant|m|}[n_oq^{(\alpha,e)}_{jj';m}(\rho_o)\alpha^{(inc)}_{j'm}+q^{(\alpha,m)}_{jj';m}(\rho_o)\tilde{\alpha}^{(inc)}_{j'm}]=\left\langle\mathbf{Y}^{(\alpha)}_{jm}{}^*(\hat{\mathbf{r}})\cdot\sum_{j'm'}[\tilde{\alpha}^{(inc)}_{j'm'}\mathbf{Q}^{(m)}_{j'm'}(\rho_o,\hat{\mathbf{r}})+n_o\alpha^{(inc)}_{j'm'}\mathbf{Q}^{(e)}_{j'm'}(\rho_o,\hat{\mathbf{r}})]\right\rangle_{\hat{\mathbf{r}}},\quad \alpha\in\{m,e\}, \tag{C4}$$

with the relations (C1), and (C2) to evaluate the left-hand side of the system (43) provided that $\{\alpha^{(c)}_{jm},\tilde{\alpha}^{(c)}_{jm}\}=\{\alpha^{(inc)}_{jm},\tilde{\alpha}^{(inc)}_{jm}\}$.

To this end, we can use Eq. (45) to write down the sum on the left-hand side of Eq. (43) in the following form:

$$\sum_{j'\geqslant|m|}\mathbf{R}^{jj';m}(r)\begin{pmatrix}\alpha^{(inc)}_{j'm}\\ \tilde{\alpha}^{(inc)}_{j'm}\end{pmatrix}=\sum_{j'\geqslant|m|}\begin{pmatrix}p^{(m,m)}_{jj';m}(\rho_o)\alpha^{(inc)}_{j'm}-n_o^{-1}p^{(m,e)}_{jj';m}(\rho_o)\tilde{\alpha}^{(inc)}_{j'm}\\ n_o\,q^{(e,e)}_{jj';m}(\rho_o)\alpha^{(inc)}_{j'm}+q^{(e,m)}_{jj';m}(\rho_o)\tilde{\alpha}^{(inc)}_{j'm}\\ n_o\,q^{(m,e)}_{jj';m}(\rho_o)\alpha^{(inc)}_{j'm}+q^{(m,m)}_{jj';m}(\rho_o)\tilde{\alpha}^{(inc)}_{j'm}\\ p^{(e,m)}_{jj';m}(\rho_o)\alpha^{(inc)}_{j'm}-n_o^{-1}p^{(e,e)}_{jj';m}(\rho_o)\tilde{\alpha}^{(inc)}_{j'm}\end{pmatrix}. \tag{C5}$$

It is seen that the elements of the column on the right-hand side of this equation are the sums from the left-hand sides of Eqs. (C3) and (C4). On the other hand, from Eqs. (C1) and (C2), the square bracketed sums on the right-hand sides of Eqs. (C3) and (C4) are the plane waves. So, the elements of the column (C5) can be evaluated as scalar products of the vector spherical functions and the vector plane waves by using Eqs. (A13) and (A14) of Appendix A.

We can now apply this procedure to calculate the elements of the column (C5) for the ordinary wave with $\{\alpha^{(inc)}_{jm},\tilde{\alpha}^{(inc)}_{jm}\}=\{\alpha^{(inc)}_{jm;y},\tilde{\alpha}^{(inc)}_{jm;y}\}$. From Eqs. (8) we have $E_x(\hat{\mathbf{k}}_{inc})=0$ and $E_y(\hat{\mathbf{k}}_{inc})=1$ in this case. The final result is

$$\sum_{j'\geqslant|m|}\mathbf{R}^{jj';m}(r)\begin{pmatrix}\alpha^{(inc)}_{j'm;y}\\ \tilde{\alpha}^{(inc)}_{j'm;y}\end{pmatrix}=\alpha^{(inc)}_{jm;y}\begin{pmatrix}j_j(\rho_o)\\ n_o[j_j(\rho_o)]'\\ 0\\ 0\end{pmatrix}+n_o^{-1}\tilde{\alpha}^{(inc)}_{jm;y}\begin{pmatrix}0\\ 0\\ n_o j_j(\rho_o)\\ -[j_j(\rho_o)]'\end{pmatrix}. \tag{C6}$$

When $n_o=n$ (and $\rho=\rho_o$), after multiplying Eq. (C6) by the matrices (46), we have

$$\sum_{j'\geqslant|m|}\mathbf{B}_{jj';m}\begin{pmatrix}\alpha^{(inc)}_{j'm;y}\\ \tilde{\alpha}^{(inc)}_{j'm;y}\end{pmatrix}=\begin{pmatrix}\alpha^{(inc)}_{jm;y}\\ n^{-1}\tilde{\alpha}^{(inc)}_{jm;y}\end{pmatrix},$$

$$\sum_{j'\geqslant|m|}\mathbf{A}_{jj';m}\begin{pmatrix}\alpha^{(inc)}_{j'm;y}\\ \tilde{\alpha}^{(inc)}_{j'm;y}\end{pmatrix}=\begin{pmatrix}0\\ 0\end{pmatrix}. \tag{C7}$$

From these equations we immediately conclude that, when $\{\alpha^{(inc)}_{jm},\tilde{\alpha}^{(inc)}_{jm}\}=\{\alpha^{(inc)}_{jm;y},\tilde{\alpha}^{(inc)}_{jm;y}\}$ and $n=n_o$, the solution of the system (47) is given by

$$\alpha^{(c)}_{jm}=\alpha^{(inc)}_{jm;y},\qquad \tilde{\alpha}^{(c)}_{jm}=\tilde{\alpha}^{(inc)}_{jm;y},$$

$$\beta^{(sca)}_{jm}\equiv\beta^{(sca)}_{jm;y}=\tilde{\beta}^{(sca)}_{jm}\equiv\tilde{\beta}^{(sca)}_{jm;y}=0. \tag{C8}$$

So, the amplitudes of scattered wave $\beta^{(sca)}_{jm;y}$ and $\tilde{\beta}^{(sca)}_{jm;y}$ vanish at $n=n_o$.

[1] G. Mie, Ann. Phys. (Leipzig) **25**, 377 (1908).
[2] S. Asano and G. Yamamoto, Appl. Opt. **14**, 29 (1975).
[3] J. Roth and M.J. Digman, J. Opt. Soc. Am. **63**, 308 (1973).
[4] B. Lange and S.R. Aragon, J. Chem. Phys. **92**, 4643 (1990).
[5] D.K. Hahn and S.R. Aragon, J. Chem. Phys. **101**, 8409 (1994).
[6] H. Karacali, S.M. Risseler, and K.F. Ferris, Phys. Rev. B **56**, 4286 (1997).
[7] A. D. Kiselev, V. Y. Reshetnyak, and T. J. Sluckin, in *Bianisotropics'2000, Proceedings of the Eighth International Conference on Electromagnetics of Complex Media, Lisbon, Portugal, 2000*, edited by A. M. Barbosa and A. L. Topa (Institute of Telecommunications, Lisbon, 2000), pp. 343–346.
[8] A.D. Kiselev, V.Y. Reshetnyak, and T.J. Sluckin, Opt. Spectrosc. **89**, 907 (2000).
[9] A. Ishimaru, *Wave Propagation and Scattering in Random Media* (Academic Press, New York, 1978).
[10] M. Kreuzer and R. Eidenschink, in *Liquid Crystals in Complex Geometries*, edited by G. P. Crawford and S. Žumer (Taylor & Francis, London, 1996), Chap. 15.
[11] T. Bellini, N.A. Clark, V. Degiorgio, F. Mantegazza, and G. Natale, Phys. Rev. E **57**, 2996 (1998).
[12] R.G. Newton, *Scattering Theory of Waves and Particles*, 2nd ed. (Springer, Heidelberg, 1982).
[13] S. Žumer and J.W. Doane, Phys. Rev. A **34**, 3373 (1986).
[14] S. Žumer, Phys. Rev. A **37**, 4006 (1988).
[15] *Light Scattering by Nonspherical Particles: Theory, Measurements and Applications*, edited by M.I. Mishchenko, J.W. Hovenier, and L.D. Travis (Academic Press, New York, 2000).
[16] M.I. Mishchenko, L.D. Travis, and D.W. Mackowski, J. Quant. Spectrosc. Radiat. Transf. **55**, 535 (1996).
[17] C.F. Boren and D.R. Huffman, *Absorption and Scattering of Light by Small Particles* (Wiley-Interscience, New York, 1983).
[18] A.D. Kiselev, V.Y. Reshetnyak, and T.J. Sluckin, e-print physics/0109022 (2001), http://arXiv.org
[19] A.D. Kiselev, V.Y. Reshetnyak, and T.J. Sluckin, e-print physics/0109023 (2001), http://arXiv.org
[20] L.C. Biedenharn and J.D. Louck, *Angular Momentum in Quantum Physics* (Addison-Wesley, Reading, MA, 1981).
[21] *Handbook of Mathematical Functions*, edited by M. Abramowitz and I. A. Stegun, (Dover, New York, 1972).
[22] I.M. Gelfand, R.A. Minlos, and Z.Y. Shapiro, *Representations of Rotation and Lorenz Groups and Their Applications* (Pergamon Press, Oxford, 1963).
[23] M. Born and E. Wolf, *Principles of Optics* 2nd ed. (Pergamon Press, Oxford, 1980).
[24] L.D. Landau and E.M. Lifshitz, *Electrodynamics of Continuous Media* (Pergamon, Oxford, 1984).
[25] M. Lax and D.F. Nelson, Phys. Rev. B **4**, 3694 (1971).
[26] H. Stark and T.C. Lubensky, Phys. Rev. E **55**, 514 (1997).
[27] D. Lacoste, B.A. van Tiggelen, G.L.J.A. Rikken, and A. Sparenberg, J. Opt. Soc. Am. A **15**, 1636 (1998).
[28] B.A. van Tiggelen, Phys. Rev. Lett. **75**, 422 (1995).
[29] G.L.J.A. Rikken and B.A. van Tiggelen, Nature (London) **381**, 54 (1996).
[30] X. Jing, P. Sheng, and M. Zhou, Phys. Rev. A **46**, 6513 (1992).
[31] C.M. Soukoulis, S. Datta, and E.N. Economou, Phys. Rev. B **49**, 3800 (1994).
[32] These computations have been performed by using the NAG FORTRAN library at the University of Southampton. The library was employed to calculate special functions, evaluate integrals and inverse matrices. In order to have the relative error well below 0.1%, the program was designed to take into account sufficiently large amounts of contributions to the scattering efficiency, which come from different angular momenta and azimuthal numbers. The detailed description of the program is beyond the scope of this paper. The code is available on request by email from any of the authors.